

Improvement of Reduced Order Modeling based on Proper Orthogonal Decomposition

Michel Bergmann, Charles-Henri Bruneau & Angelo Iollo

`Michel.Bergmann@inria.fr`
`http://www.math.u-bordeaux.fr/~bergmann/`

INRIA Bordeaux Sud-Ouest
Institut de Mathématiques de Bordeaux
351 cours de la Libération
33405 TALENCE cedex, France

Summary

Context and flow configuration

I - A pressure extended Reduced Order Model based on POD

- ▶ Proper Orthogonal Decomposition (POD)
- ▶ Reduced Order Model (ROM)

II - Stabilization of reduced order models

- ▶ Residuals based stabilization method
- ▶ Classical SUPG and VMS methods

III - Improvement of the functional subspace

- ▶ Krylov like method
- ▶ An hybrid DNS/POD ROM method (Database modification)

Conclusions

Context and flow configuration

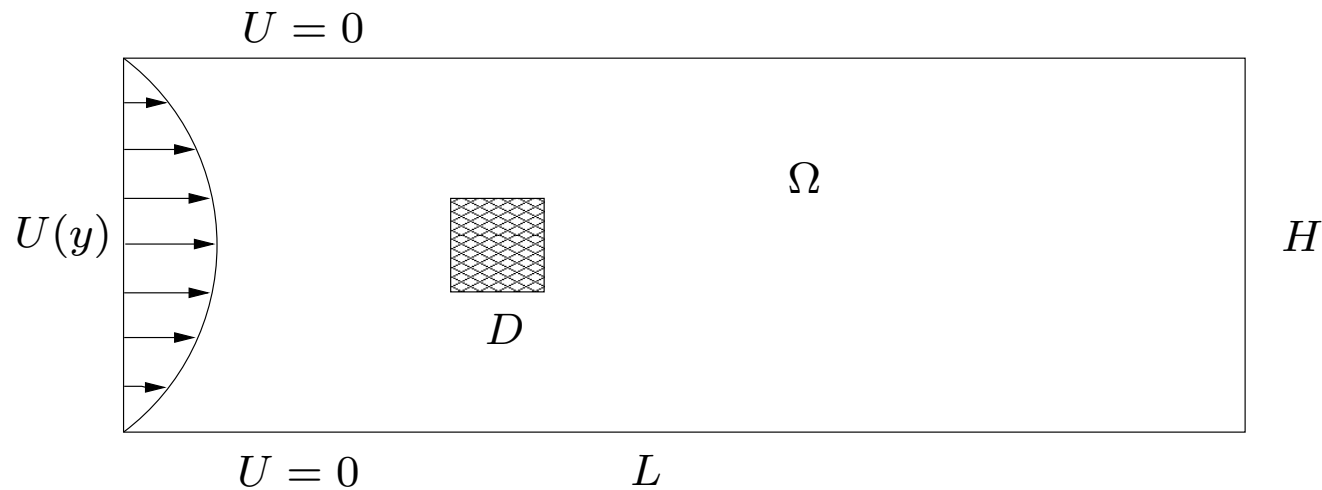
▷ Context

- Need of reduced order model for flow control purpose
 - ↔ To reduce the CPU time
 - ↔ To reduce the memory storage during adjoint-based minimization process
- Optimization + POD ROM methods
 - ↔ Generalized basis, no POD basis actualization : fast but no "convergence" proof
 - ↔ Trust Region POD (TRPOD), POD basis actualization : proof of convergence !
- Drawbacks
 - ↔ Need to stabilize POD ROM (lack of dissipation, numerical issues, pressure term)
 - ↔ Basis actualization : DNS → high numerical costs !
- Solutions
 - ↔ Efficient ROM & stabilization
 - ↔ Low costs functional subspace adaptation during optimization process

Context and flow configuration

▷ Flow Configuration

- 2-D Confined flow past a square cylinder in laminar regime
- Viscous fluid, incompressible and newtonian
- No control



▷ Numerical methods

- Penalization method for the square cylinder
- Multigrids V-cycles method in space
- Gear method in time

C.-H. Bruneau solver

I - A pressure extended Reduced Order Model

Proper Orthogonal Decomposition (POD), Lumley (1967)

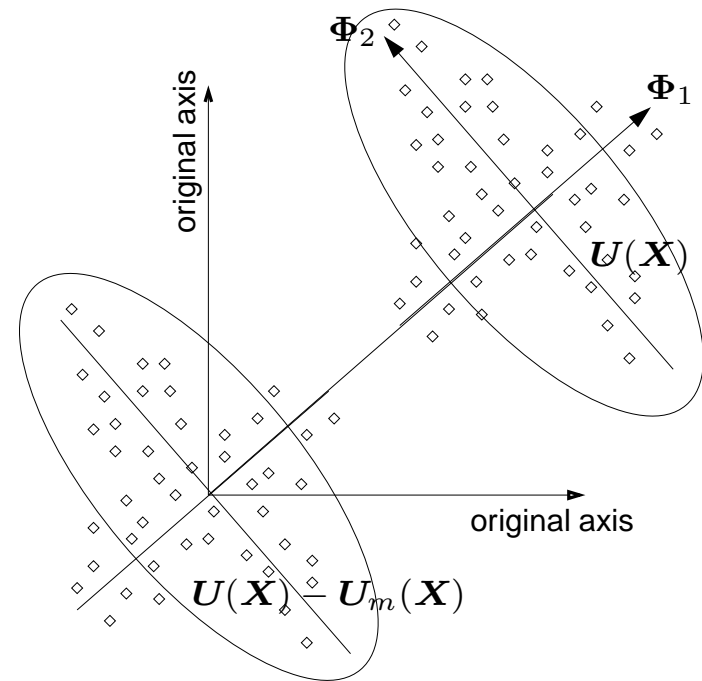
- ▷ Look for the flow realization $\Phi(\mathbf{X})$ that is "the closest" in an average sense to realizations $\mathbf{U}(\mathbf{X})$.

$$(\mathbf{X} = (\mathbf{x}, t) \in \mathcal{D} = \Omega \times \mathbb{R}^+)$$

- ▷ $\Phi(\mathbf{X})$ solution of problem :

$$\max_{\Phi} \langle |(\mathbf{U}, \Phi)|^2 \rangle, \quad \|\Phi\|^2 = 1.$$

- ▷ Optimal convergence in L^2 norm de $\Phi(\mathbf{X})$
 \Rightarrow Dynamical reduction possible.



Lumley J.L. (1967) : The structure of inhomogeneous turbulence. *Atmospheric Turbulence and Wave Propagation*, ed. A.M. Yaglom & V.I. Tatarski, pp. 166-178.

I - A pressure extended Reduced Order Model

- ▷ Equivalent with Fredholm equation :

$$\int_{\mathcal{D}} R_{ij}(\mathbf{X}, \mathbf{X}') \Phi_n^{(j)}(\mathbf{X}') d\mathbf{X}' = \lambda_n \Phi_n^{(i)}(\mathbf{X}) \quad n = 1, \dots, N_s$$

$\hookrightarrow R(\mathbf{X}, \mathbf{X}') : \text{Space-time correlation tensor}$

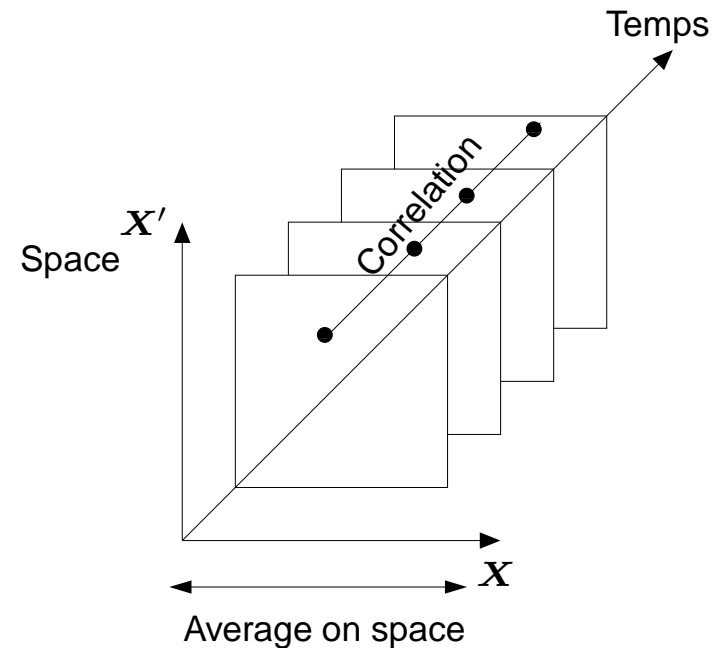
- ▷ Snapshots method, Sirovich (1987) :

$$\int_T C(t, t') a_n(t') dt' = \lambda_n a_n(t)$$

$\hookrightarrow C(t, t') : \text{Temporal correlations}$

- ▷ $\Phi(\mathbf{X})$ flow basis :

$$\mathbf{U}(\mathbf{x}, t) = \sum_{n=1}^{N_s} a_n(t) \Phi_n(\mathbf{x}).$$



Sirovich L. (1987) : Turbulence and the dynamics of coherent structures. Part 1,2,3 *Quarterly of Applied Mathematics*, **XLV** N° 3, pp. 561–571.

I - A pressure extended Reduced Order Model

Truncation of the POD basis to keep 99% of the Relative Information Content

$$RIC(M) = \frac{\sum_{k=1}^M \lambda_k}{\sum_{k=1}^{N_s} \lambda_k}$$

Example at $Re = 200$ for $\mathbf{U} = (\mathbf{u}, p)^T$ with $N_s = 200$

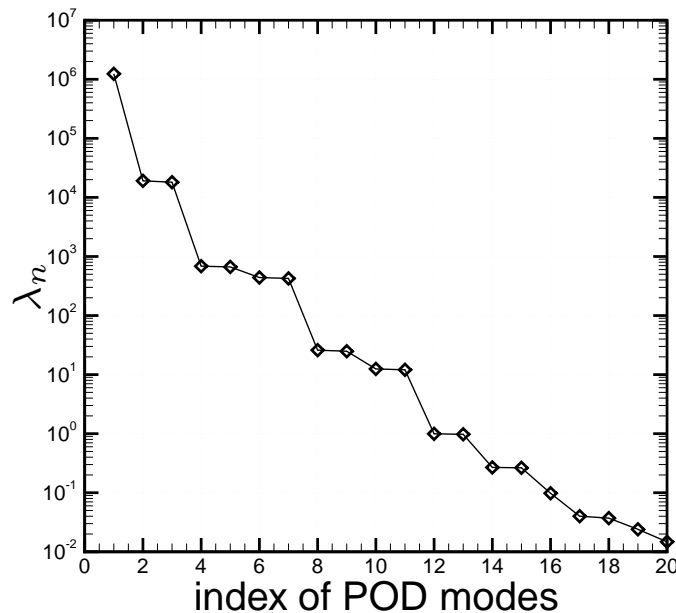


Fig. : *POD spectrum.*

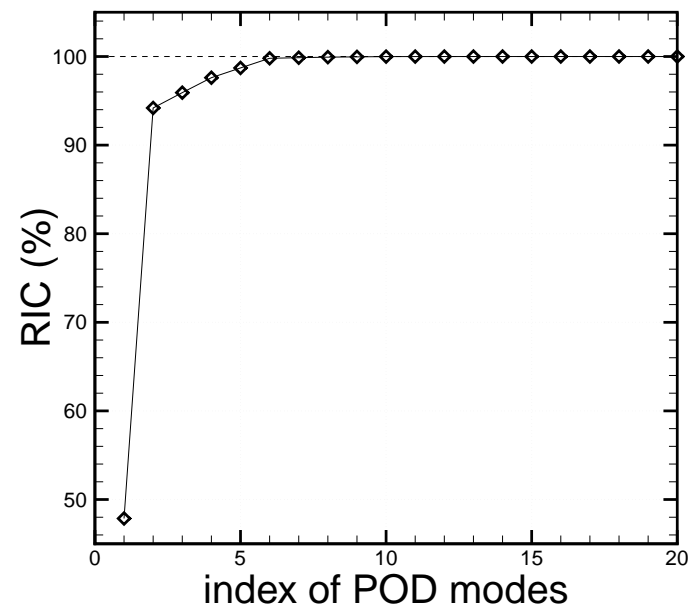


Fig. : *RIC(M), M nb modes POD retenus.*

$$N_r = \arg \min_M RIC(M) \text{ s.t. } RIC(N_r) > 99\% \Rightarrow N_r = 5!$$

I - A pressure extended Reduced Order Model

The POD basis is $\Phi = (\phi, \psi)^T$

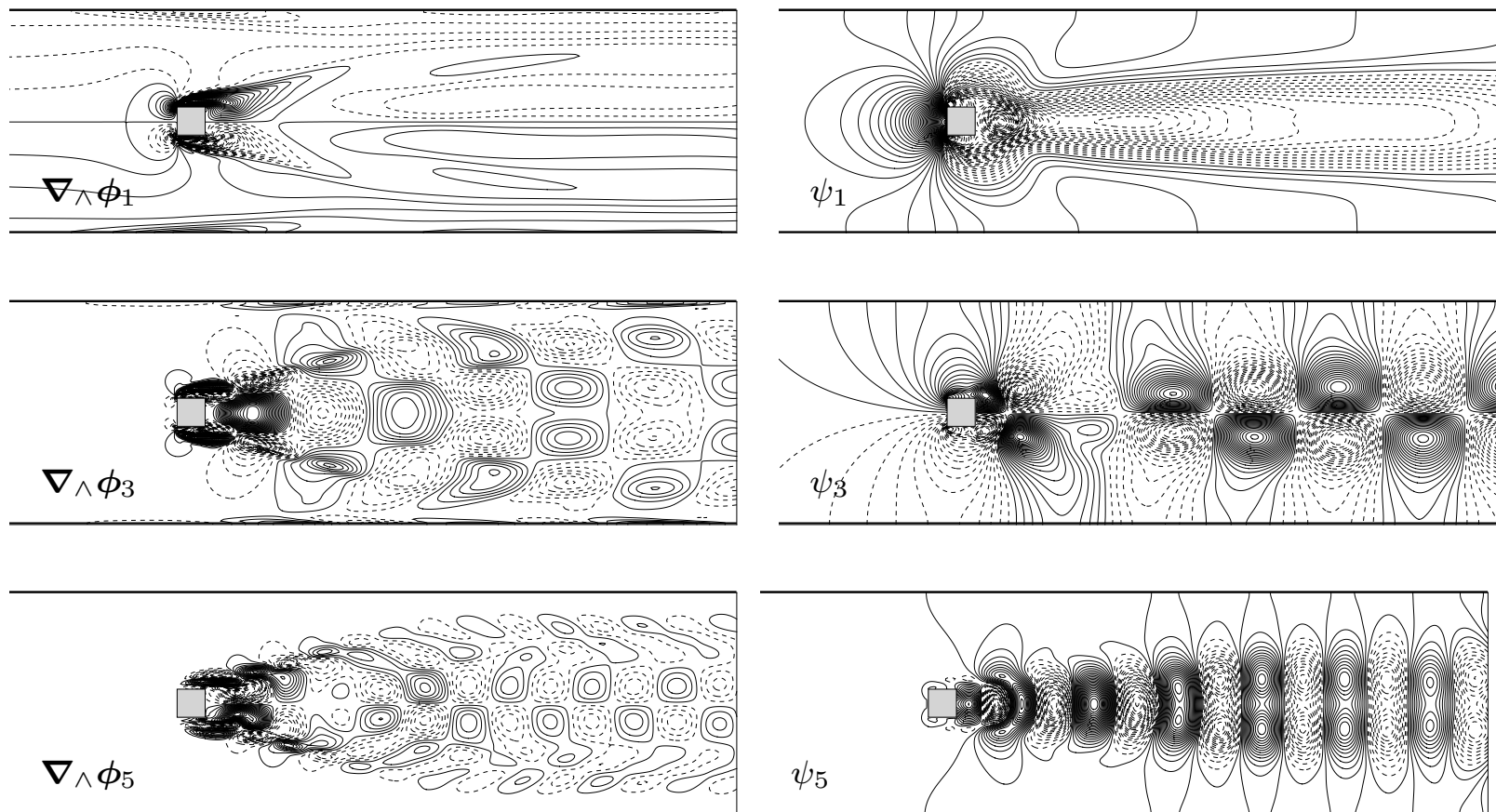


Fig. : Representation of some POD modes. Iso-vorticity (left) and isobars (right). Dashed lines represent negative values (the pressure reference is arbitrarily chosen to be zero)

I - A pressure extended Reduced Order Model

► Momentum conservation

Detailed model (exact)

$$\frac{\partial \mathbf{u}}{\partial t} + (\mathbf{u} \cdot \nabla) \mathbf{u} = -\nabla p + \frac{1}{Re} \Delta \mathbf{u}$$

Galerkin projection using $\tilde{\mathbf{u}}(\mathbf{x}, t) = \sum_{i=1}^{N_r} a_i(t) \phi_i(\mathbf{x})$ and $\tilde{p}(\mathbf{x}, t) = \sum_{i=1}^{N_r} a_i(t) \psi_i(\mathbf{x})$:

$$\left(\phi_i, \sum_{j=1}^{N_r} \phi_j \frac{da_j}{dt} + \sum_{j=1}^{N_r} \sum_{k=1}^{N_r} (\phi_j \cdot \nabla) \phi_k a_j a_k + \sum_{j=1}^{N_r} \nabla \psi_j a_j - \frac{1}{Re} \sum_{j=1}^{N_r} \Delta \phi_j a_j \right)_{\Omega} = 0.$$

The Reduced Order Model is then :

$$\sum_{j=1}^{N_r} L_{ij}^{(m)} \frac{da_j}{dt} = \sum_{j=1}^{N_r} B_{ij}^{(m)} a_j + \sum_{j=1}^{N_r} \sum_{k=1}^{N_r} C_{ijk}^{(m)} a_j a_k$$

↔ The ROM does not satisfy *a priori* the mass conservation
(for non divergence free modes, as NSE-Residual modes)

I - A pressure extended Reduced Order Model

► Mass conservation

Detailed model

$$\nabla \cdot \mathbf{u} = 0$$

Projection onto the POD basis

$$\sum_{j=1}^{N_r} a_j \nabla \cdot \phi_j = 0$$

Minimizing residuals in a least squares sense, we obtain :

$$\sum_{j=1}^{N_r} B_{ij}^{(c)} a_j = 0, \quad \text{where} \quad B_{ij}^{(c)} = (\nabla \cdot \phi_j)^T \nabla \cdot \phi_j$$

The modified ROM that satisfies both momentum and continuity equation writes :

$$\sum_{j=1}^{N_r} L_{ij}^{(m)} \frac{da_j}{dt} = \sum_{j=1}^{N_r} \left(B_{ij}^{(m)} + \alpha B_{ij}^{(c)} \right) a_j + \sum_{j=1}^{N_r} \sum_{k=1}^{N_r} C_{ijk}^{(m)} a_j a_k$$

↪ The ROM has moreover to satisfy the flow rate conservation.

I - A pressure extended Reduced Order Model

► Flow rate conservation

For the 2-D confined flow :

$$\int_{\mathcal{S}} u \, ds = c,$$

For each slides \mathcal{S}_l :

$$\sum_{j=1}^{N_r} a_j(t) \int_{\mathcal{S}_l} \phi_j^u \, ds = c,$$

$$\sum_{j=1}^{N_r} \frac{da_j}{dt} \int_{\mathcal{S}_l} \phi_j^u \, ds = 0.$$

In a least square sense :

$$\sum_{j=1}^{N_r} L_{ij}^{(r)} \frac{da_j}{dt} = 0.$$

Finally, the ROM writes

$$\sum_{j=1}^{N_r} \left(L_{ij}^{(m)} + \beta L_{ij}^{(r)} \right) \frac{da_j}{dt} = \sum_{j=1}^{N_r} \left(B_{ij}^{(m)} + \alpha B_{ij}^{(c)} \right) a_j + \sum_{j=1}^{N_r} \sum_{k=1}^{N_r} C_{ijk}^{(m)} a_j a_k,$$

with initial conditions $a_i(0) = (\mathbf{U}(\mathbf{x}, 0), \Phi_i(\mathbf{x}))_{\Omega} \quad i = 1, \dots, N_r.$

I - A pressure extended Reduced Order Model

► Advantage no modelisation of the pressure term

$Re = 200$, 11 modes \Rightarrow convergence towards the exact limit cycles (= DNS)

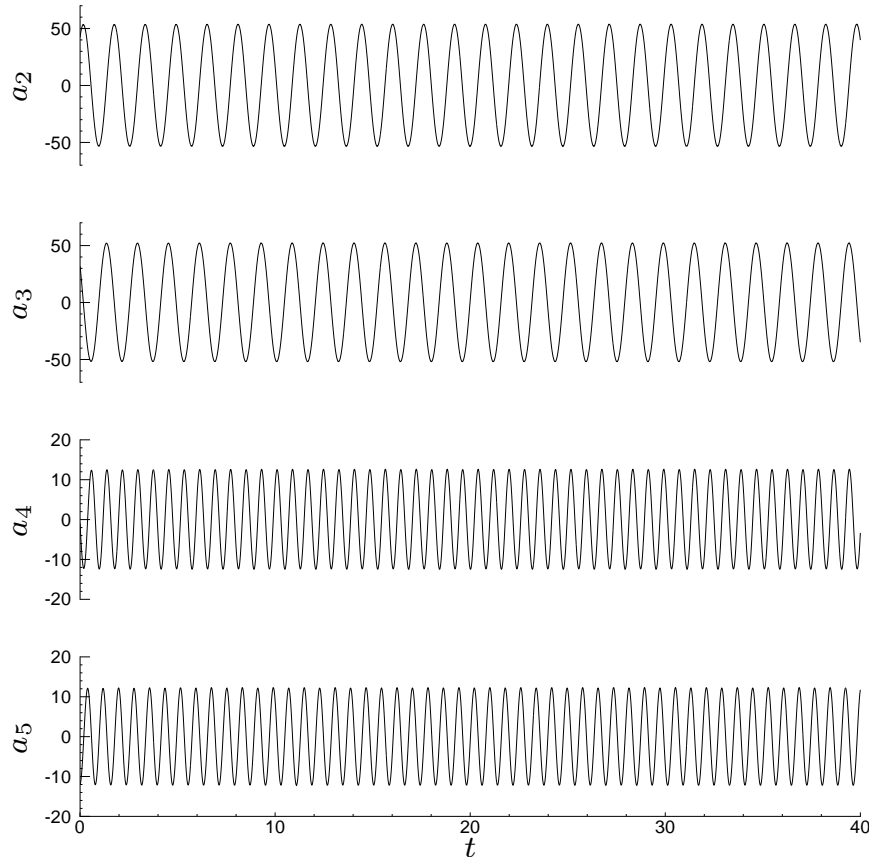


Fig. : Temporal evolution of the POD ROM coefficients over 25 vortex shedding periods

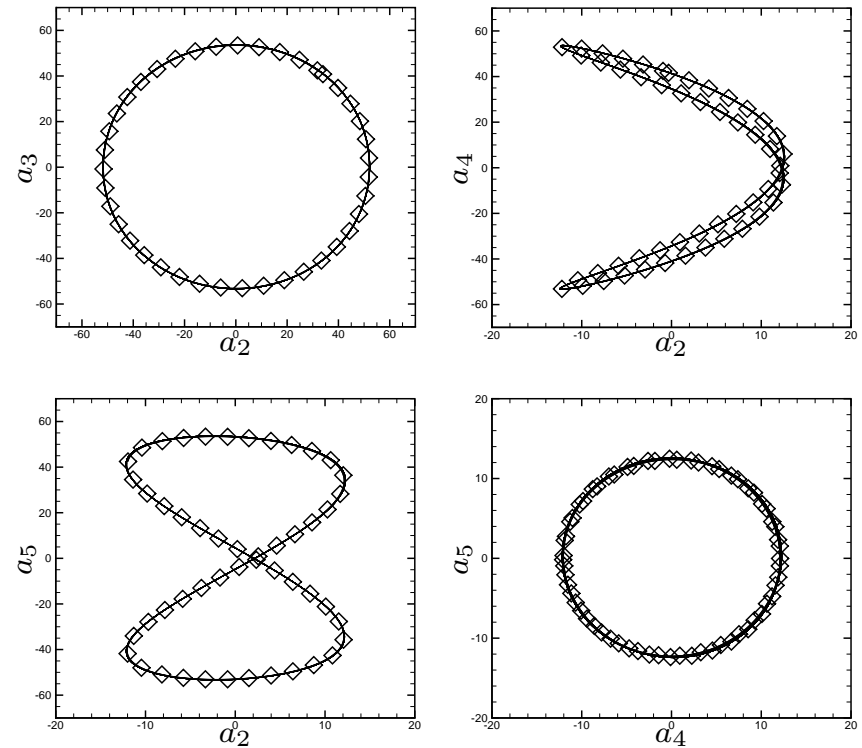


Fig. : Limit cycles of the POD ROM coefficients over 25 vortex shedding periods

I - A pressure extended Reduced Order Model

► Drawbacks same as usual, *i.e.* lack of dissipation...

$Re = 200$, 5 modes \Rightarrow convergence towards an erroneous limit cycles (\neq DNS)

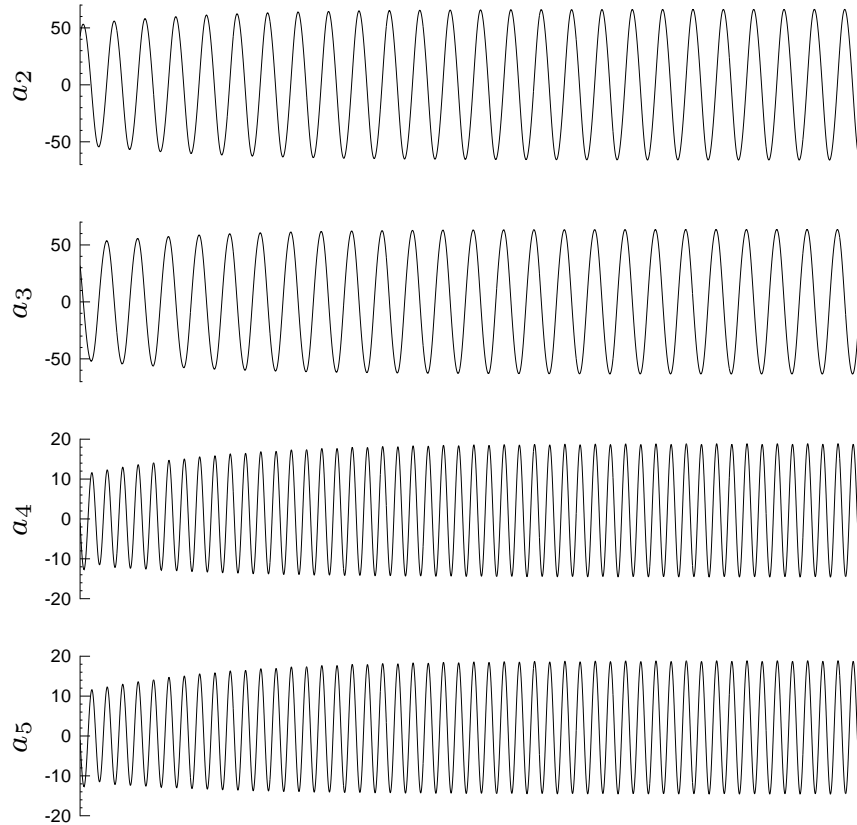


Fig. : Temporal evolution of the POD ROM coefficients over 25 vortex shedding periods

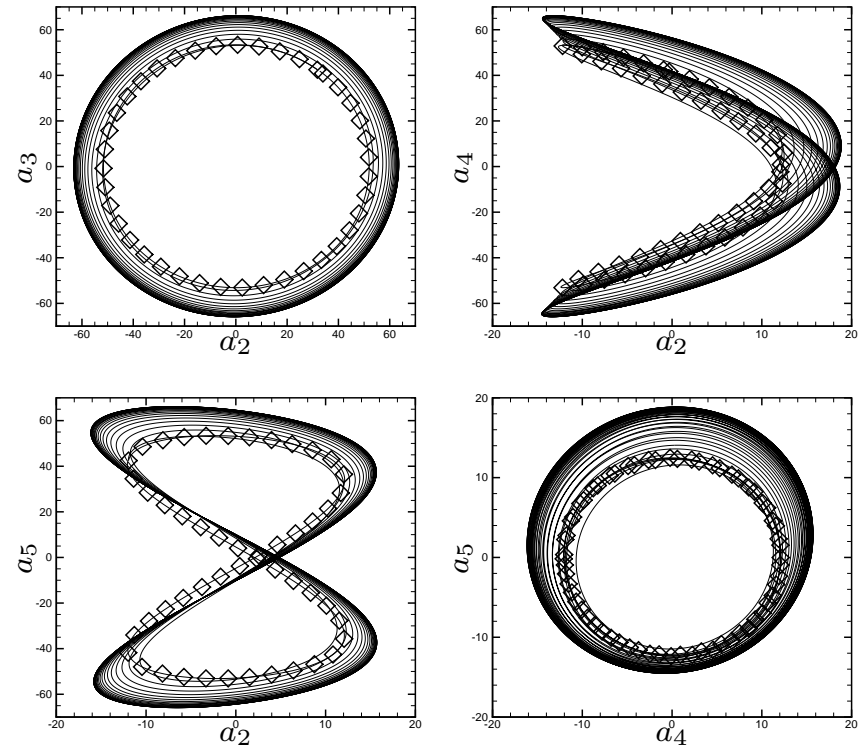


Fig. : Limit cycles of the POD ROM coefficients over 25 vortex shedding periods

I - A pressure extended Reduced Order Model

► Drawbaks same as usual, *i.e.* lack of dissipation...

$Re = 200$, 3 modes \Rightarrow exponential divergence

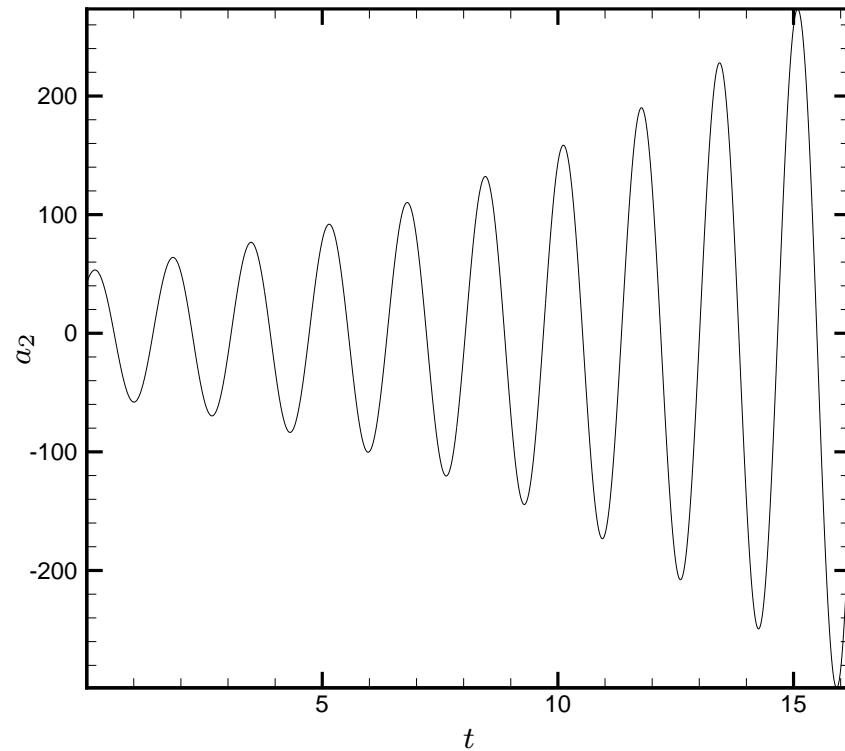


Fig. : Temporal evolution of the POD ROM coefficients over 25 vortex shedding periods

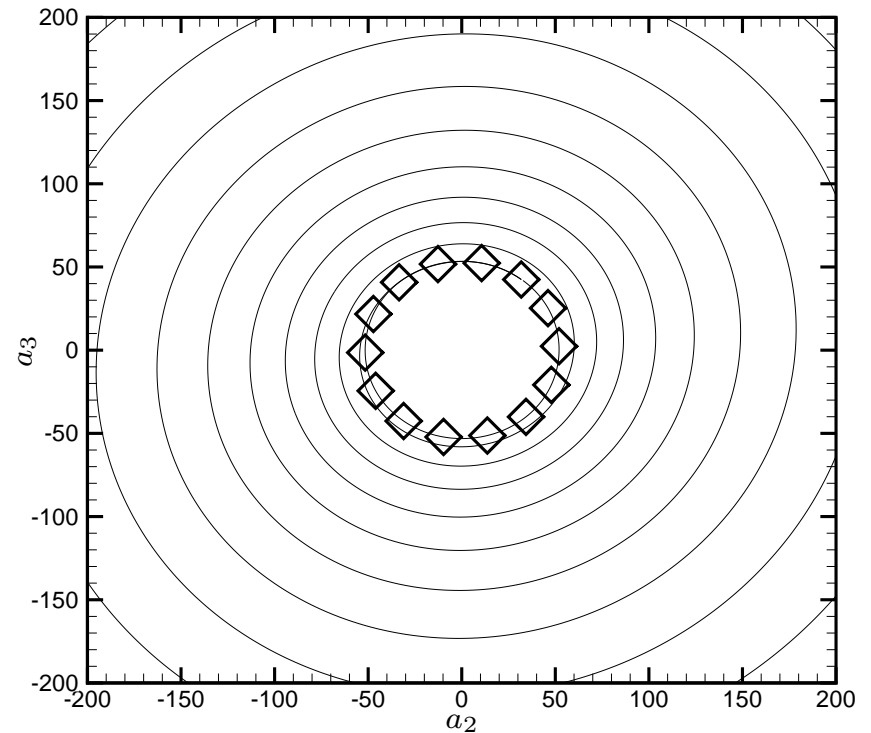


Fig. : Limit cycles of the POD ROM coefficients over 25 vortex shedding periods

II - POD ROM stabilization

► Overview of stabilization methods (non-exhaustive)

● Eddy viscosity

↳ Heisenberg viscosity

↳ Spectral vanishing viscosity

↳ Optimal viscosity

● Penalty method

● Calibration of POD ROM coefficients

► "New" stabilization methods in POD ROM context

● *Residuals based stabilization method*

● *Streamline Upwind Petrov-Galerkin (SUPG) and Variational Multi-scale (VMS) methods*

II - POD ROM stabilization

► Residuals based stabilization method

⇒ **Idea** add dominant POD-NSE residual modes to the existing basis

↪ The POD-NSE residuals are $\mathcal{L}(\tilde{\mathbf{u}}(\mathbf{x}, t), \tilde{p}(\mathbf{x}, t)) = \mathbf{R}(\mathbf{x}, t)$,
where $\tilde{\mathbf{u}}$ and \tilde{p} obtained using POD and \mathcal{L} is the NSE operator

● **Model $A^{[N_r]}$** , unstable POD ROM built with N_r basis functions $\Phi_i(\mathbf{x})$.

Algorithm

1. Integrate the ROM to obtain $a_i(t)$ and extract N_s snapshots $a_i(t_k)$, $k = 1, \dots, N_s$.

2. Compute $\tilde{\mathbf{u}}(\mathbf{x}, t_k) = \sum_{i=1}^{N_r} a_i(t_k) \phi_i(\mathbf{x})$, $\tilde{p}(\mathbf{x}, t_k) = \sum_{i=1}^{N_r} a_i(t_k) \psi_i(\mathbf{x})$, and $\mathbf{R}(\mathbf{x}, t_k)$.

3. Compute the POD modes $\Psi(\mathbf{x})$ of the NSE residuals.

4. Add the K first residual modes $\Psi(\mathbf{x})$ to the existing POD basis $\Phi_i(\mathbf{x})$ and build a new ROM (here the mass and flow rate constraints are important).

● **Model $B^{[N_r;K]}$** , PODRES ROM built with N_r POD basis functions $\Phi_i(\mathbf{x})$
+ K RES basis functions $\Psi_i(\mathbf{x})$

II - POD ROM stabilization

► SUPG and VMS methods

⇒ **Idea** approximate the fine scales using the NSE residuals $\mathbf{R} = (\mathbf{R}_M, R_C)^T$

$$\mathbf{u}'(\mathbf{x}, t) = \tau_M \mathbf{R}_M(\mathbf{x}, t) \quad \text{and} \quad p'(\mathbf{x}, t) = \tau_C R_C(\mathbf{x}, t)$$

↪ Class of penalty methods, *i.e.*

$$\sum_{j=1}^{N_r} L_{ij} \frac{da_j}{dt} = \sum_{j=1}^{N_r} B_{ij} a_j + \sum_{j=1}^{N_r} \sum_{k=1}^{N_r} C_{ijk} a_j a_k + F_i(t)$$

● **Model $C^{[N_r]}$, SUPG method**

$$F_i^{SUPG}(t) = (\tilde{\mathbf{u}} \cdot \nabla \Phi_i + \nabla \Psi_i, \tau_M \mathbf{R}_M(\mathbf{x}, t))_{\Omega} + (\nabla \cdot \Phi_i, \tau_C R_C(\mathbf{x}, t))_{\Omega}$$

● **Model $D^{[N_r]}$, VMS method**

$$F_i^{VMS}(t) = F_i^{SUPG}(t) + (\tilde{\mathbf{u}} \cdot (\nabla \Phi_i)^T, \tau_M \mathbf{R}_M(\mathbf{x}, t))_{\Omega} \\ - (\nabla \Phi_i, \tau_M \mathbf{R}_M(\mathbf{x}, t) \otimes \tau_M \mathbf{R}_M(\mathbf{x}, t))_{\Omega}$$

↪ Parameters τ_M and τ_C are determined using adjoint based minimization method

II - POD ROM stabilization

► $Re = 200$ and $N_r = 5$ POD basis function → erroneous limit cycles

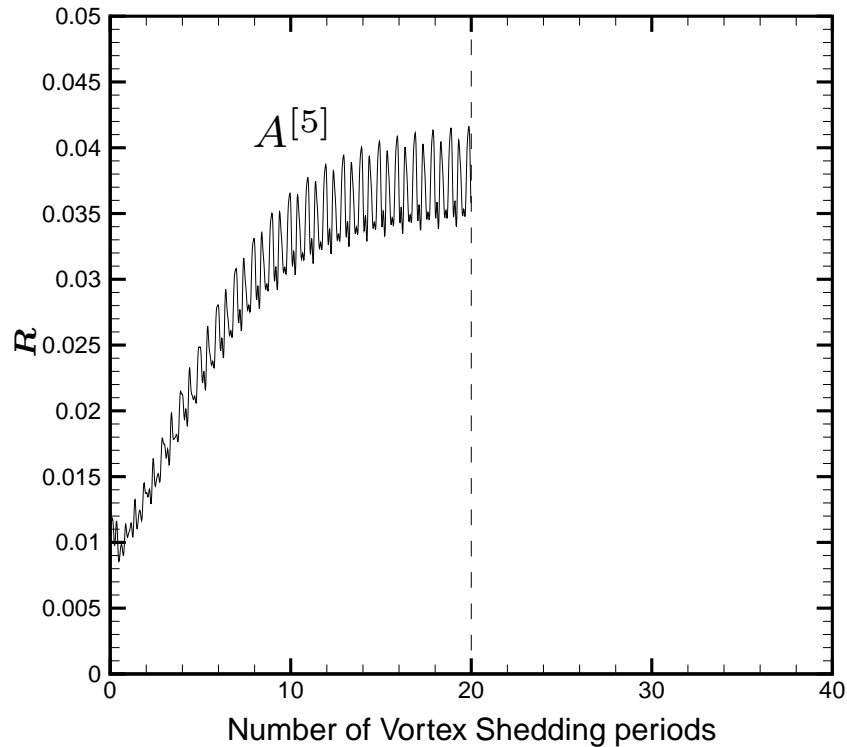


Fig. : temporal evolution of the L_2 norm of the POD-NSE residuals

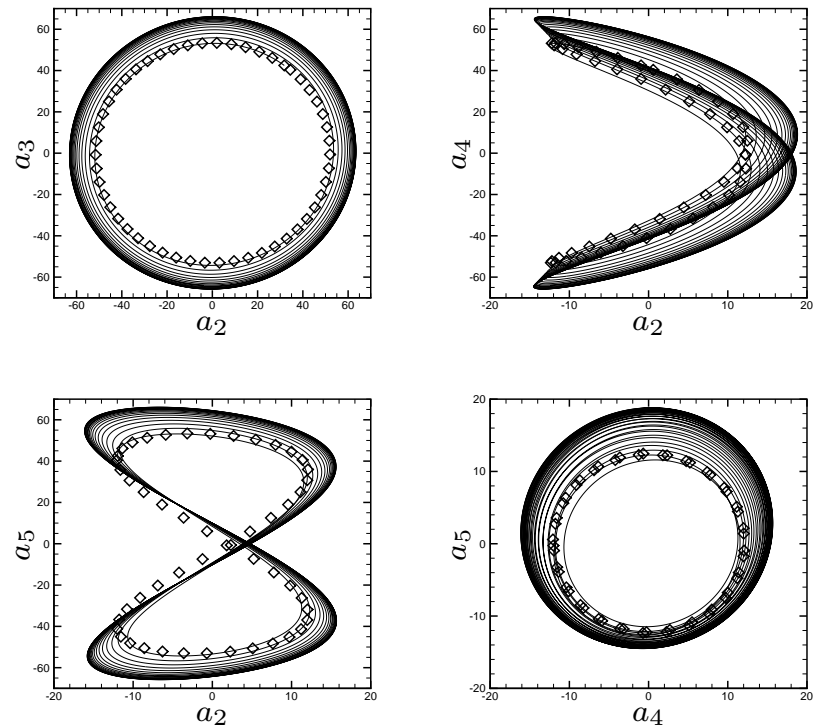


Fig. : Limit cycles of the POD ROM coefficients over 20 vortex shedding periods

II - POD ROM stabilization

► $Re = 200$ and $N_r = 5$ POD basis function → erroneous limit cycles

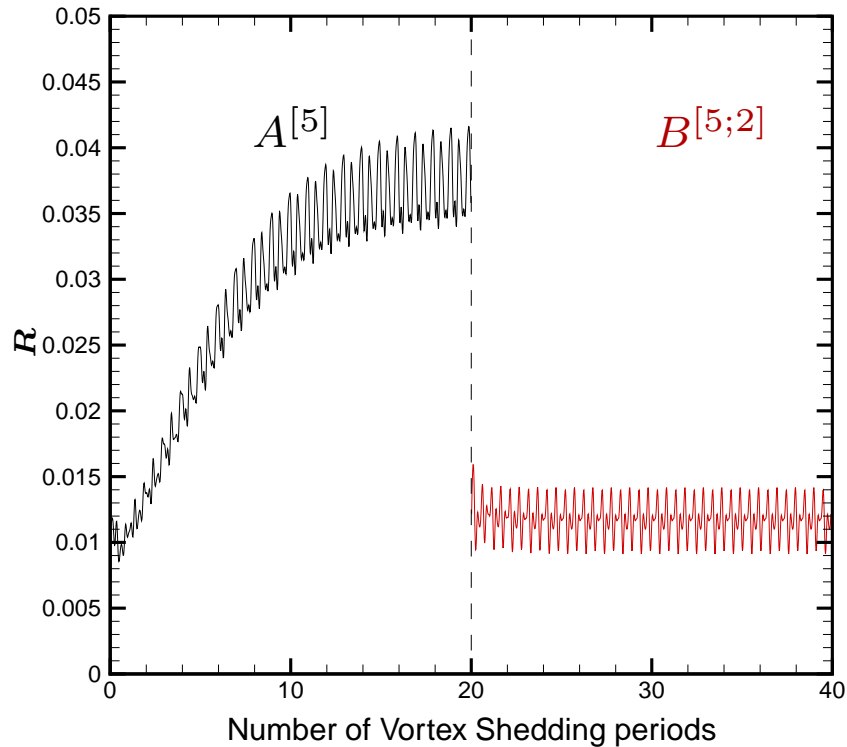


Fig. : temporal evolution of the L_2 norm of the POD-NSE residuals

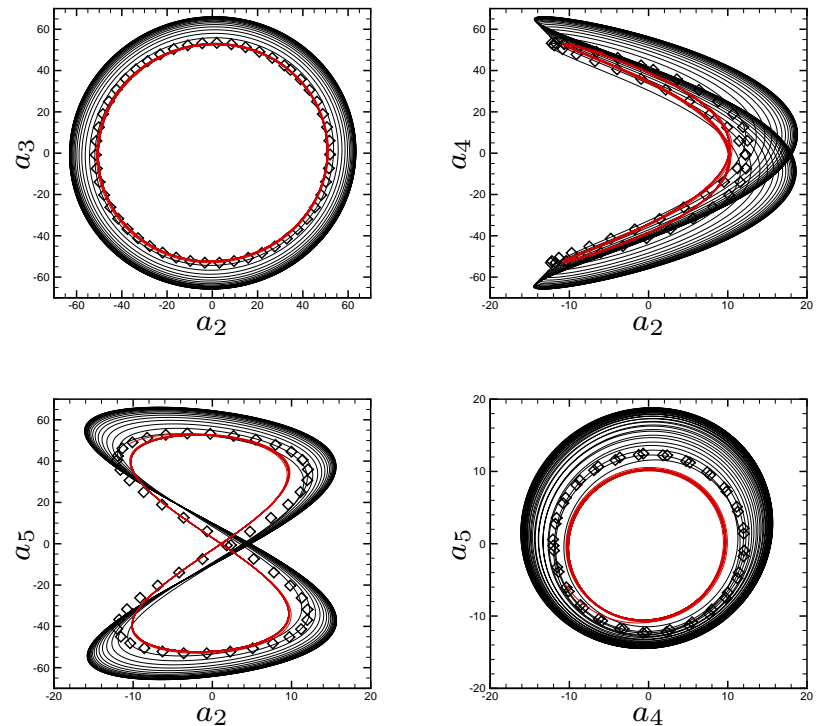


Fig. : Limit cycles of the POD ROM coefficients over 20 vortex shedding periods

II - POD ROM stabilization

► $Re = 200$ and $N_r = 5$ POD basis function → erroneous limit cycles

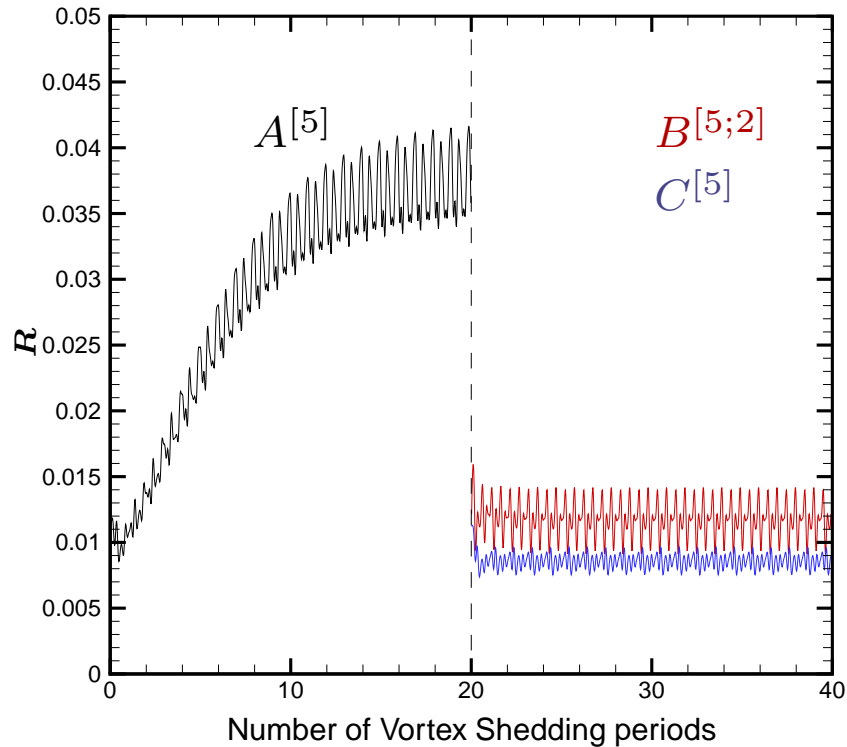


Fig. : temporal evolution of the L_2 norm of the POD-NSE residuals

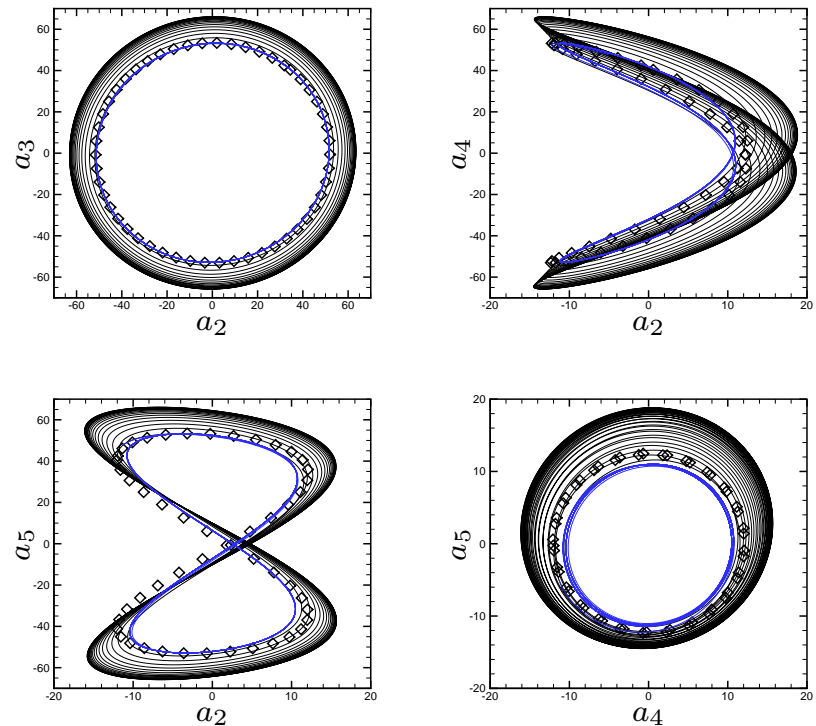


Fig. : Limit cycles of the POD ROM coefficients over 20 vortex shedding periods

II - POD ROM stabilization

► $Re = 200$ and $N_r = 5$ POD basis function → erroneous limit cycles

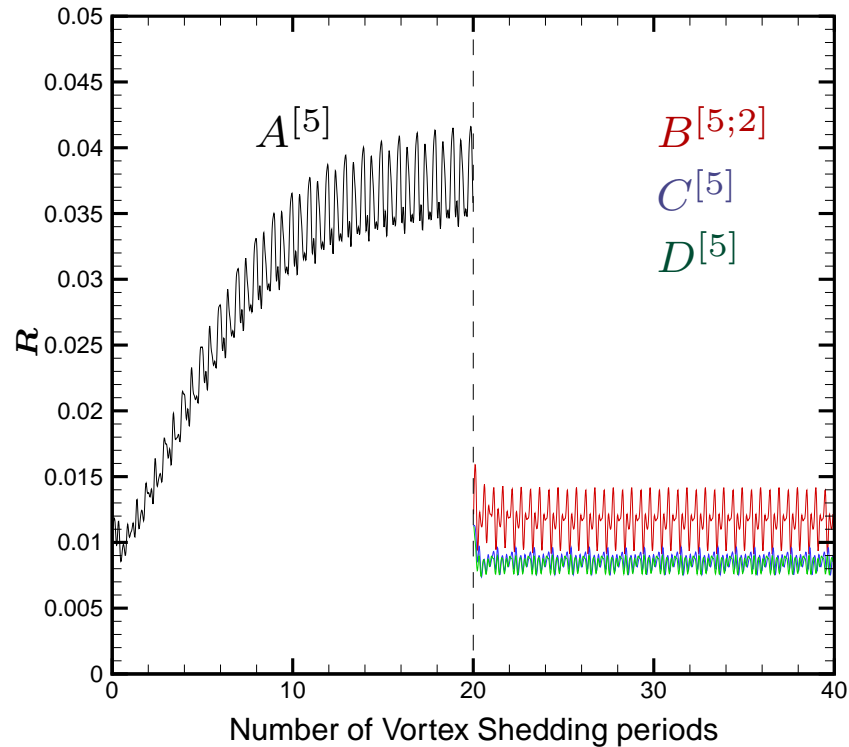


Fig. : temporal evolution of the L_2 norm of the POD-NSE residuals

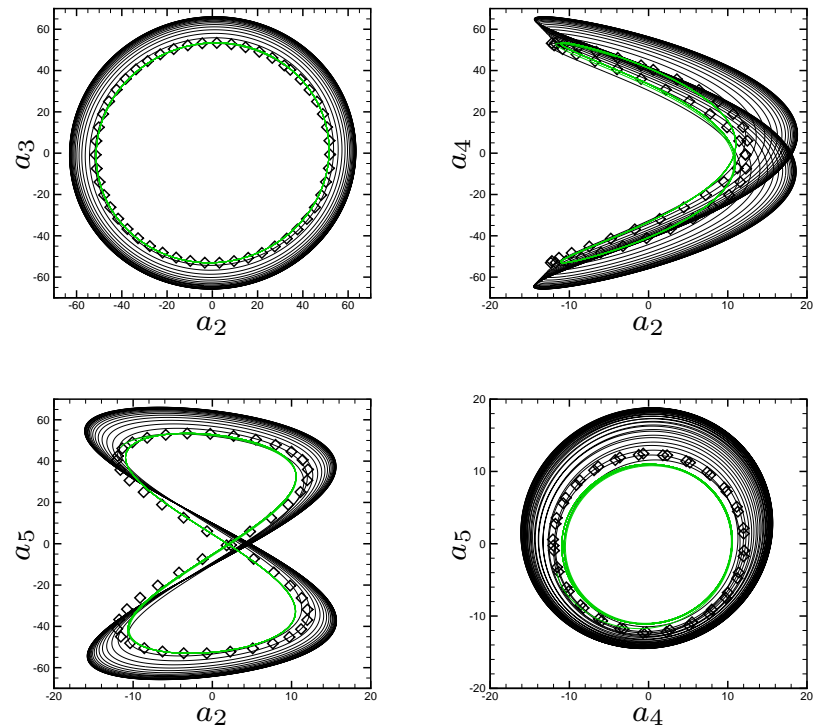


Fig. : Limit cycles of the POD ROM coefficients over 20 vortex shedding periods

II - POD ROM stabilization

► $Re = 200$ and $N_r = 3$ POD basis function → divergence

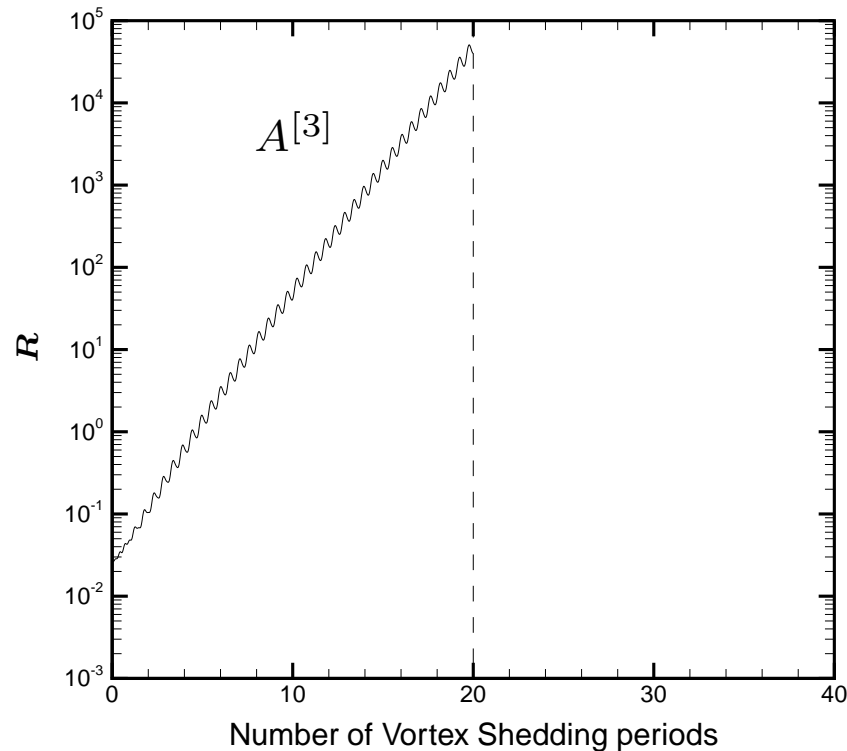


Fig. : temporal evolution of the L_2 norm of the POD-NSE residuals

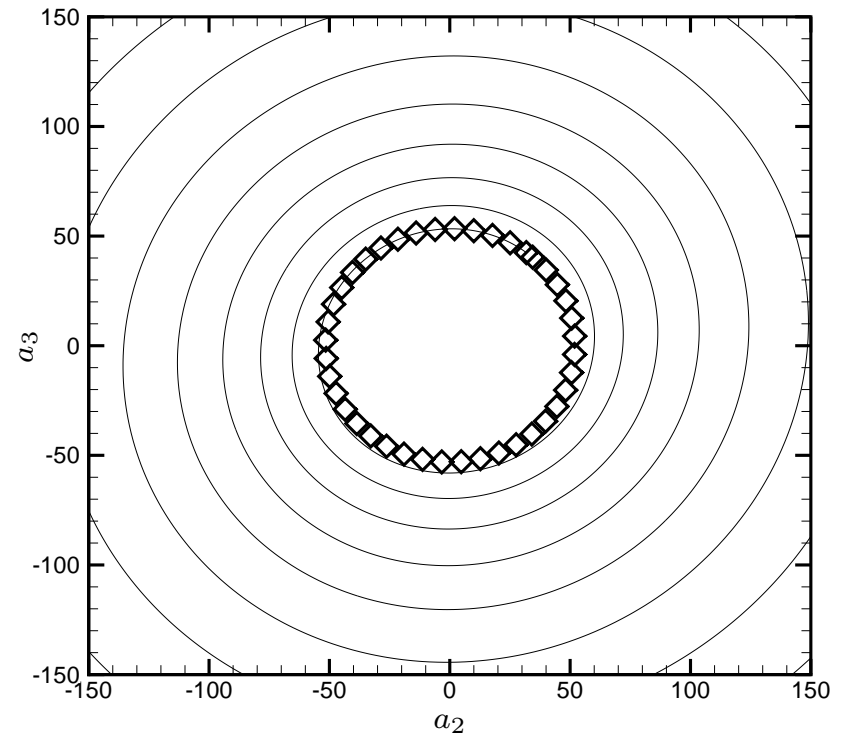


Fig. : Limit cycle of the POD ROM coefficients over 20 vortex shedding periods

II - POD ROM stabilization

► $Re = 200$ and $N_r = 3$ POD basis function → divergence

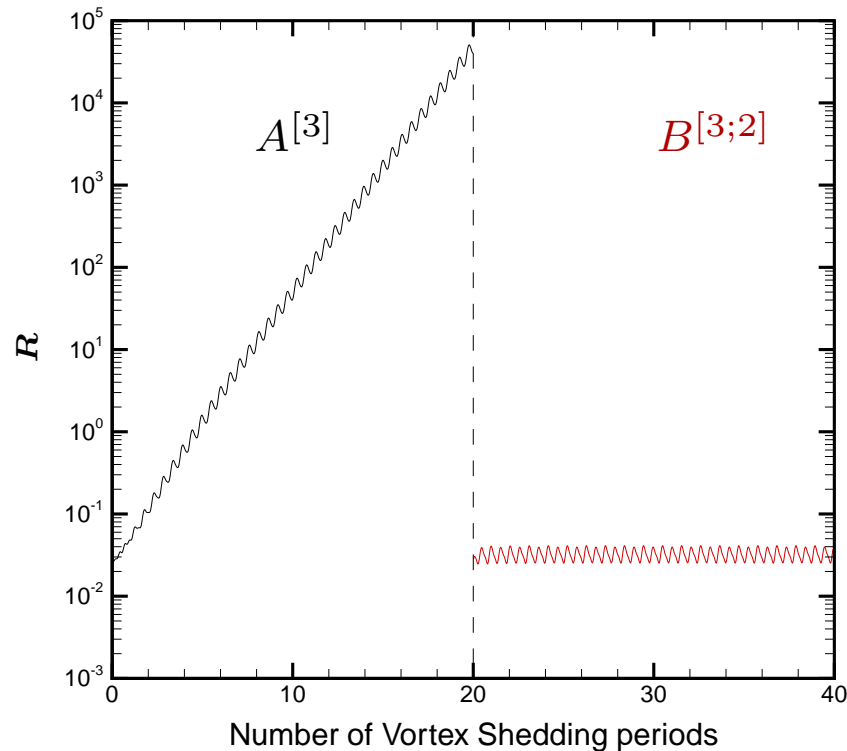


Fig. : temporal evolution of the L_2 norm of the POD-NSE residuals

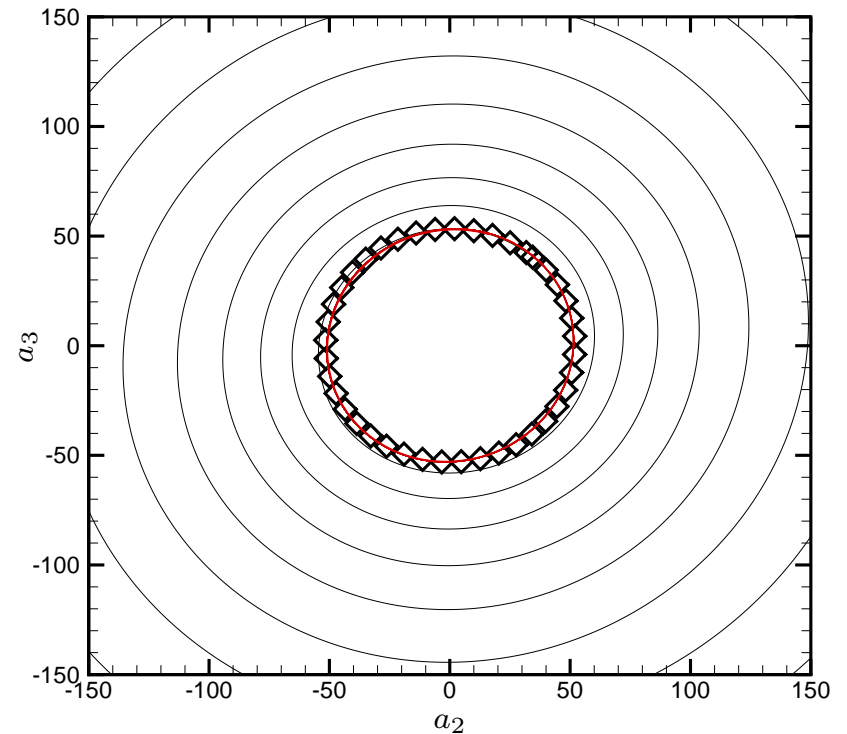


Fig. : Limit cycle of the POD ROM coefficients over 20 vortex shedding periods

II - POD ROM stabilization

► $Re = 200$ and $N_r = 3$ POD basis function → divergence

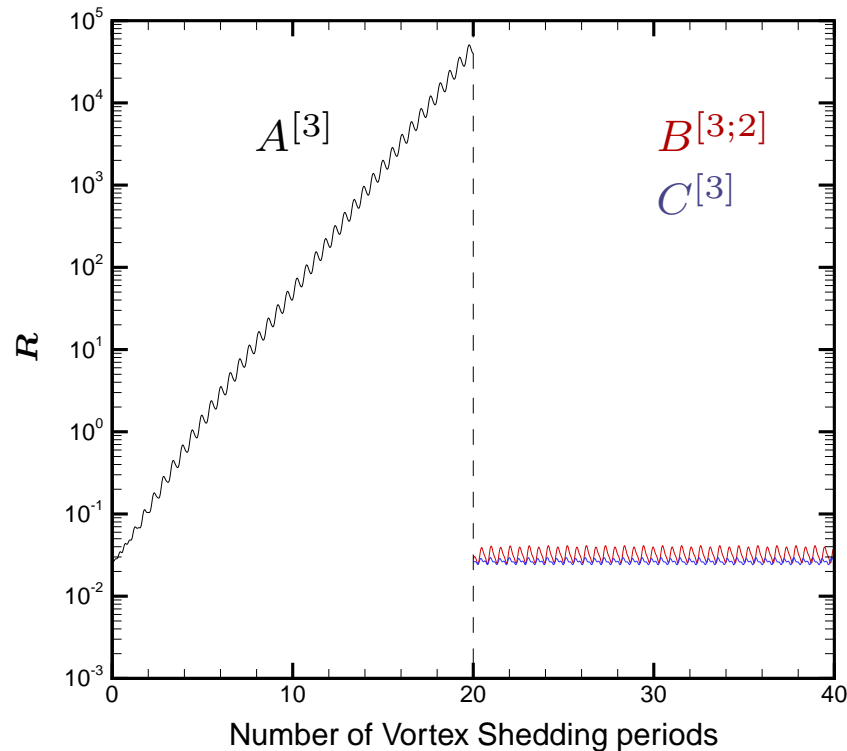


Fig. : temporal evolution of the L_2 norm of the POD-NSE residuals

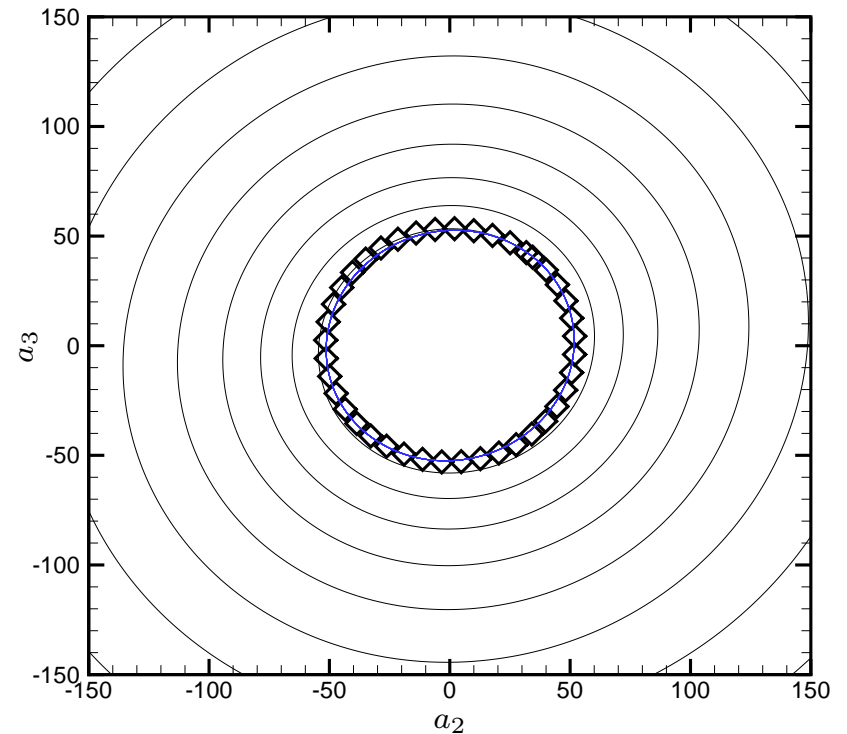


Fig. : Limit cycle of the POD ROM coefficients over 20 vortex shedding periods

II - POD ROM stabilization

► $Re = 200$ and $N_r = 3$ POD basis function → divergence

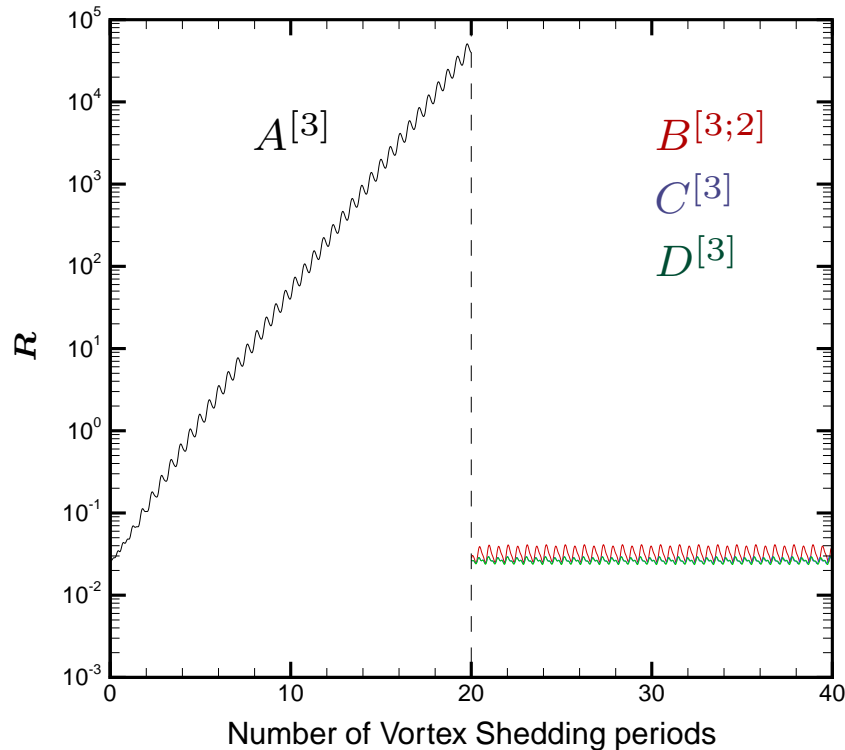


Fig. : temporal evolution of the L_2 norm of the POD-NSE residuals

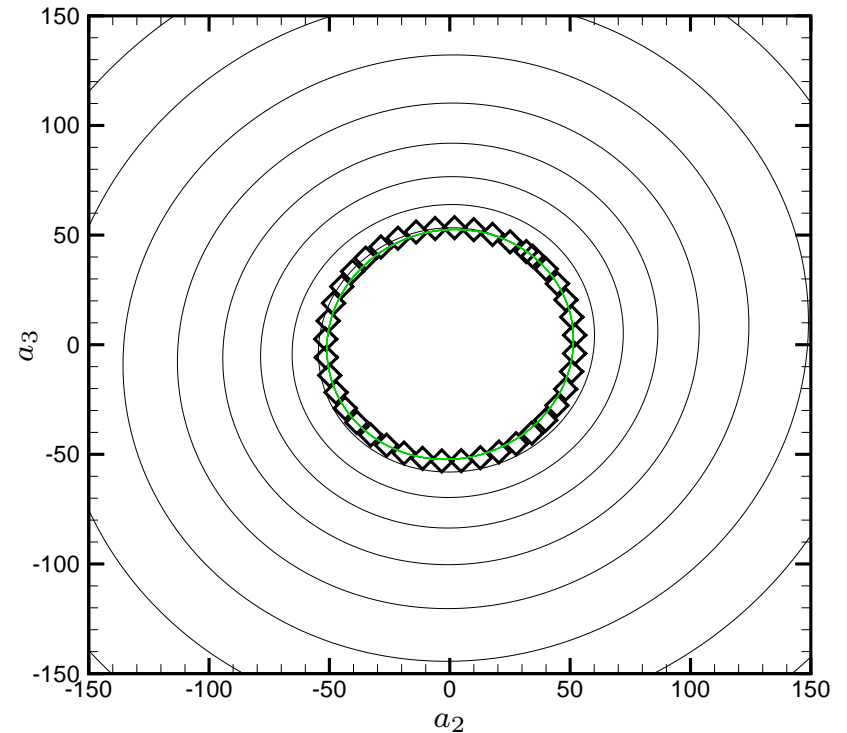
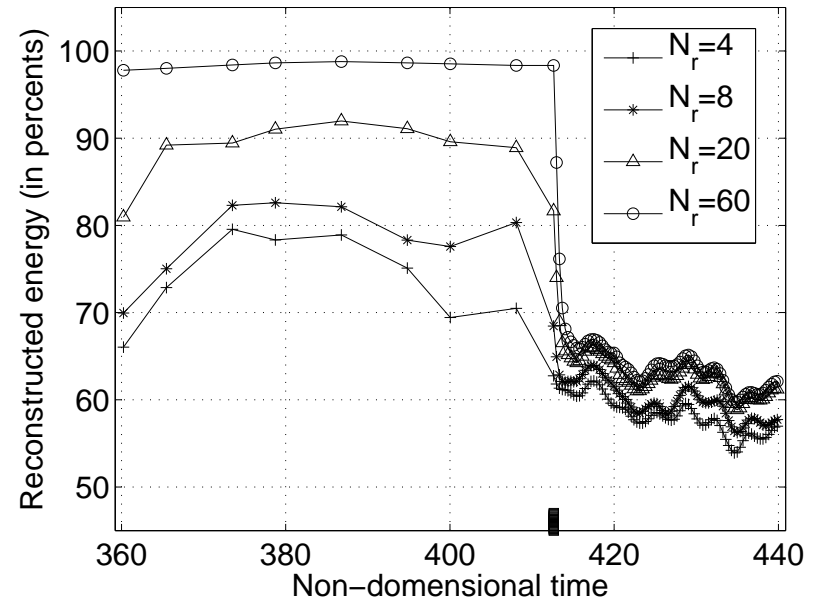
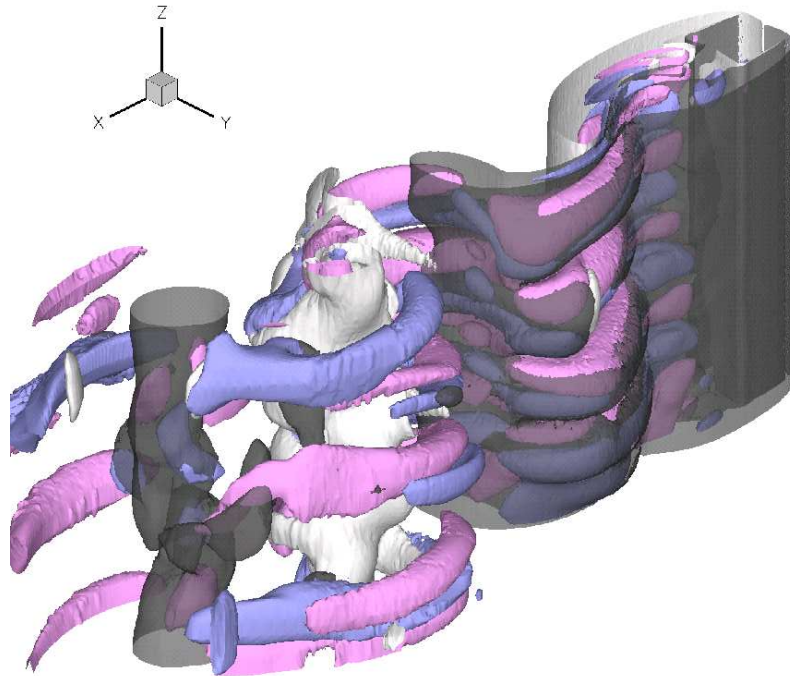


Fig. : Limit cycle of the POD ROM coefficients over 20 vortex shedding periods

III - Improvement of the functional subspace

- **Functional subspace drawbacks, $\Phi_n(x)$** : lack of representativity of 3D flows *outside the database*



Figures results from Buffoni *etal.* Journal of Fluid Mech. **569** (2006)

- Problems for 3D flow control
- Erroneous turbulence properties (spectrum, *etc*)

⇒ **Goal : determine $\Phi_n(x)$ at Re_2 starting from $\Phi_n(x)$ at Re_1 for low numerical costs.**

III - Improvement of the functional subspace

▷ Method 1 : Krylov-like method to improve the functional subspace $\Phi_n(\mathbf{x})$

- **Use of the POD-NSE residuals** : $\mathcal{L}(\tilde{\mathbf{u}}(\mathbf{x}, t), \tilde{\mathbf{p}}(\mathbf{x}, t)) = \mathbf{R}(\mathbf{x}, t)$,
 $\tilde{\mathbf{u}}$ and $\tilde{\mathbf{p}}$ are POD fields, \mathcal{L} is the NSE operator

Algorithm

Start with the POD basis to be improved, Φ_i with $i = 1, \dots, N_r$. Let $N_0 = N_r$.

1. Build and solve the corresponding ROM to obtain $a_i(t)$ and extract N_s snapshots $a_i(t_k)$ with $i = 1, \dots, N_r$ and $k = 1, \dots, N_s$.

2. Compute $\tilde{\mathbf{u}}(\mathbf{x}, t_k) = \sum_{i=1}^{N_r} a_i(t_k) \phi_i(\mathbf{x})$, $\tilde{\mathbf{p}}(\mathbf{x}, t_k) = \sum_{i=1}^{N_r} a_i(t_k) \psi_i(\mathbf{x})$, and $\mathbf{R}(\mathbf{x}, t_k)$.

3. Compute the POD modes $\Psi(\mathbf{x})$ of the NSE residuals.

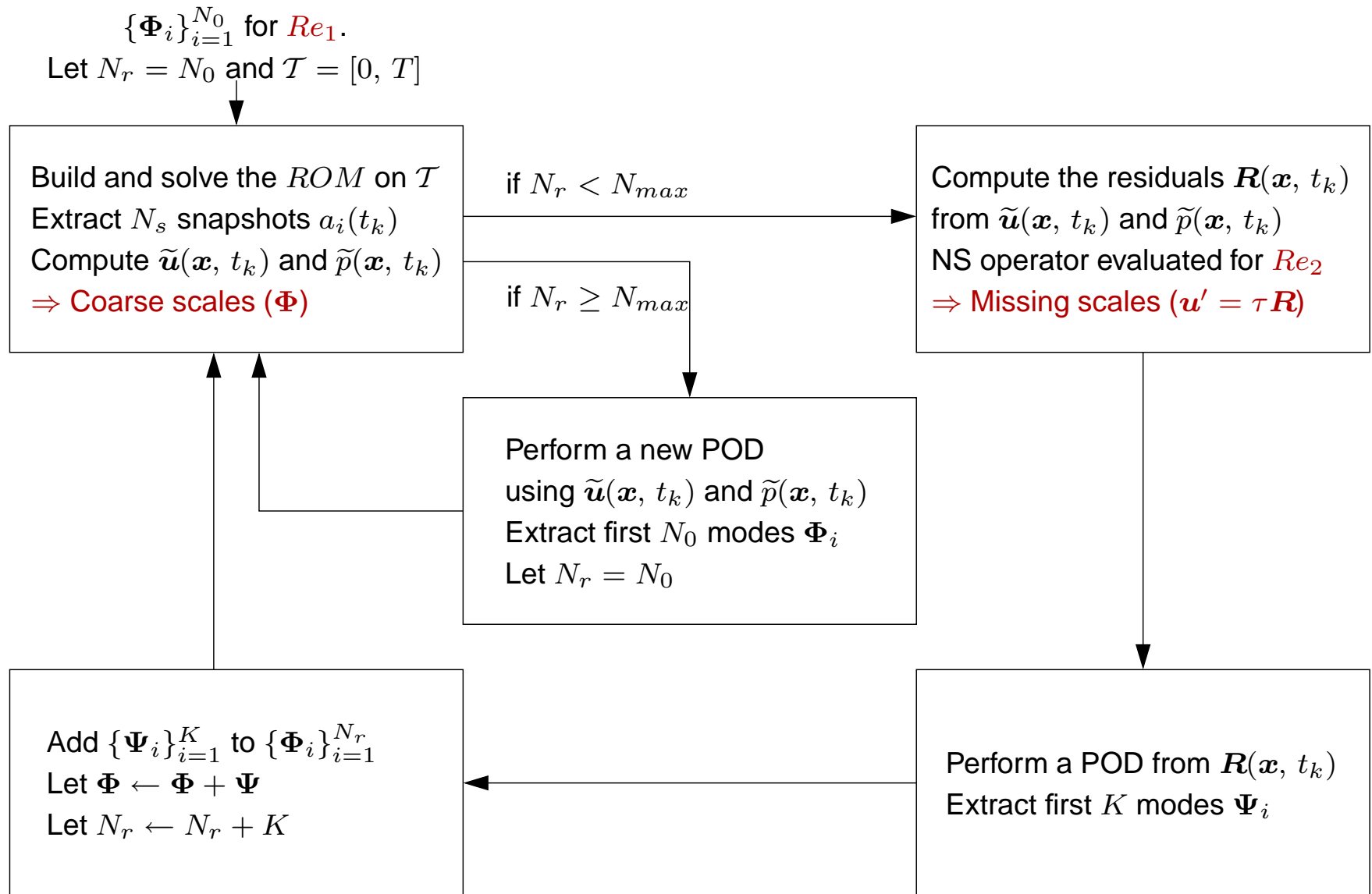
4. Add the K first residual modes $\Psi(\mathbf{x})$ to the existing POD basis $\Phi_i(\mathbf{x})$

- $\Phi \leftarrow \Phi + \Psi$
- $N_r \leftarrow N_r + K$
- If N_r is below than a threshold, return to 1. Else, go to 5.

5. Perform a new POD compression with $N_r = N_0$.

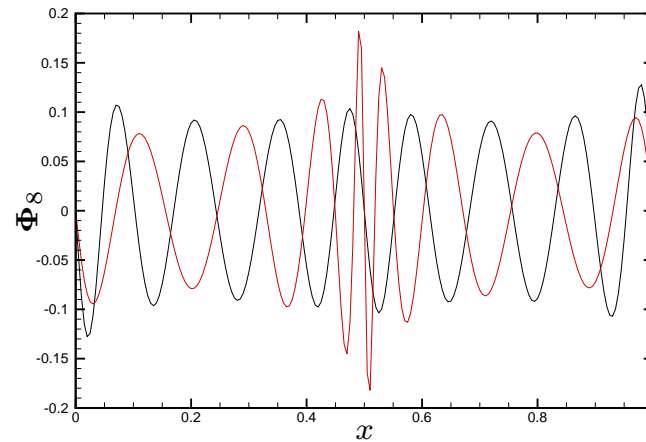
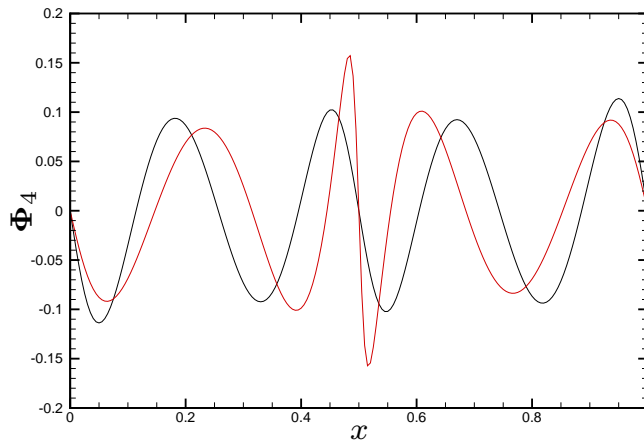
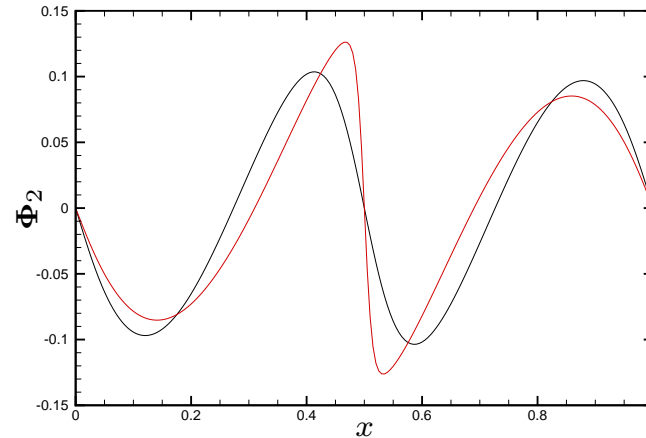
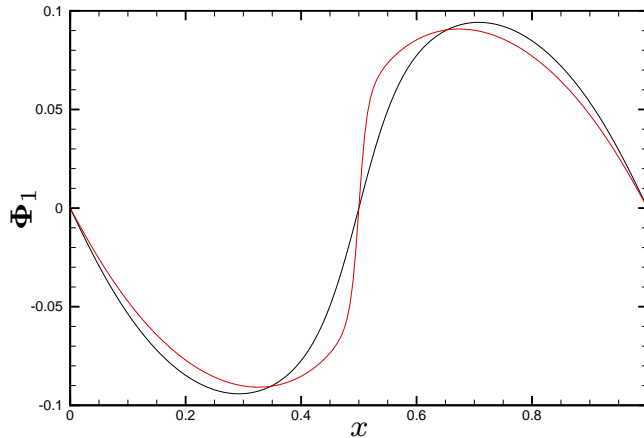
- If convergence is satisfied, stop. Else, return to 1.

III - Improvement of the functional subspace



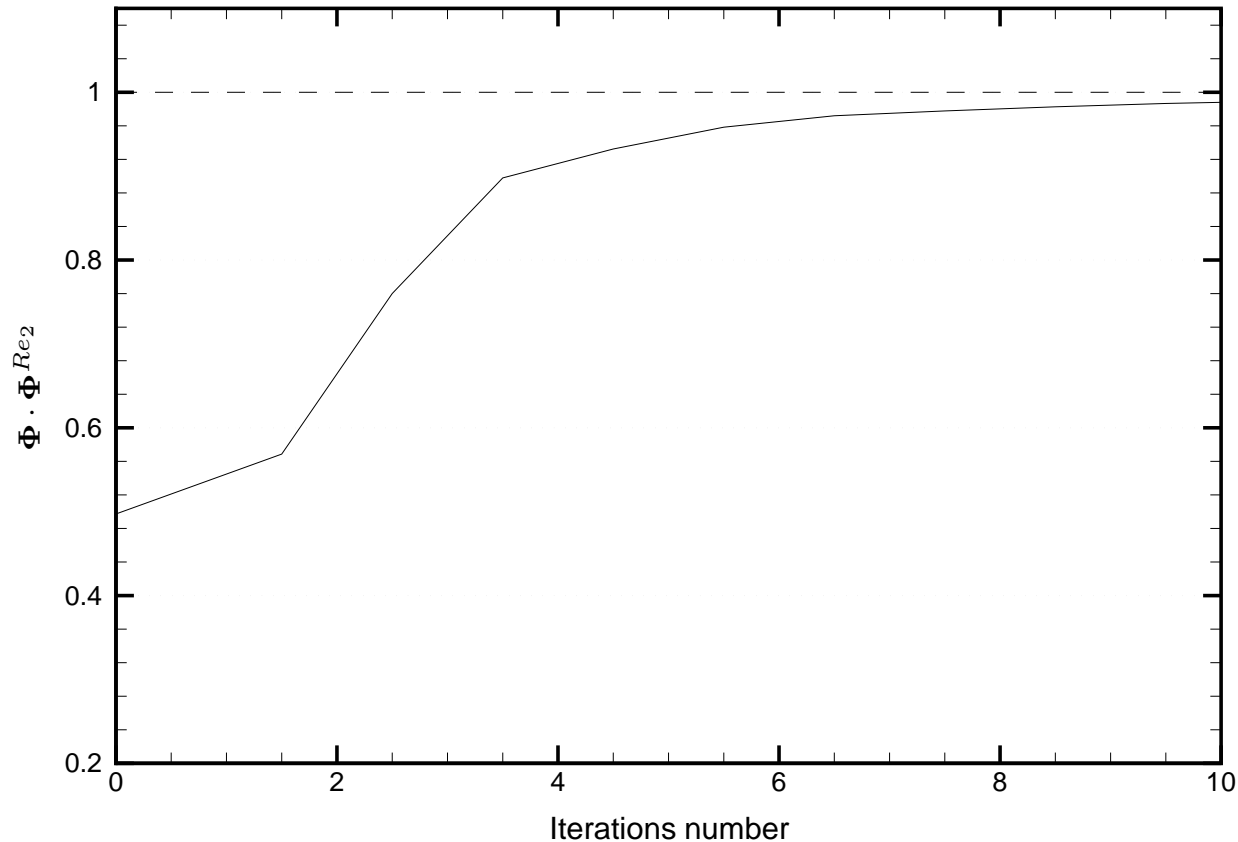
III - Improvement of the functional subspace

► First test case : 1D burgers equation $Re_1 = 50 \rightarrow Re_2 = 300$ ($\Phi^{Re_1} \cdot \Phi^{Re_2} \approx 0.5$)



III - Improvement of the functional subspace

► First test case : 1D burgers equation $Re_1 = 50 \rightarrow Re_2 = 300$ ($\Phi^{Re_1} \cdot \Phi^{Re_2} \approx 0.5$)

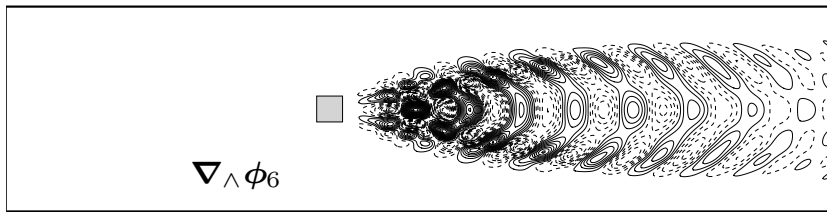
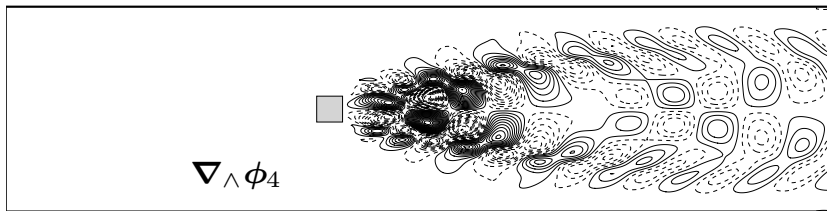
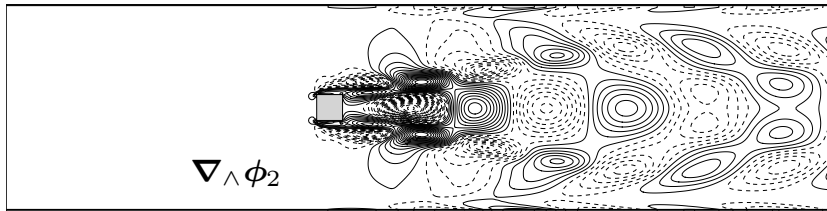
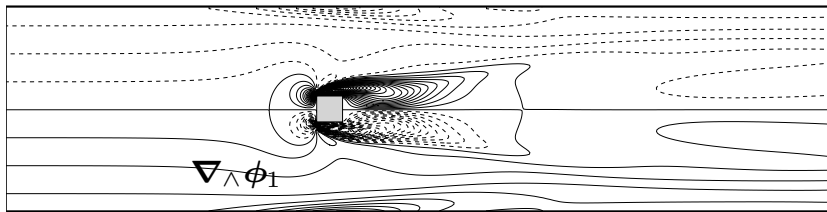


↪ Only 6 ROM integrations (on $T = 1$) are necessary to converge (no DNS!!)

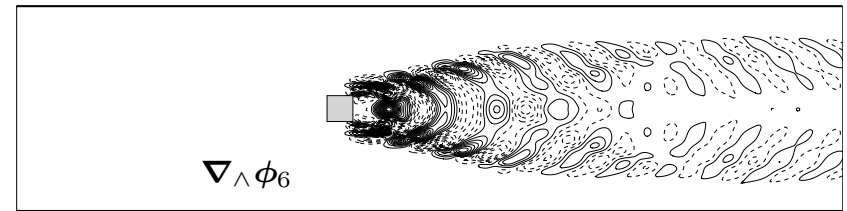
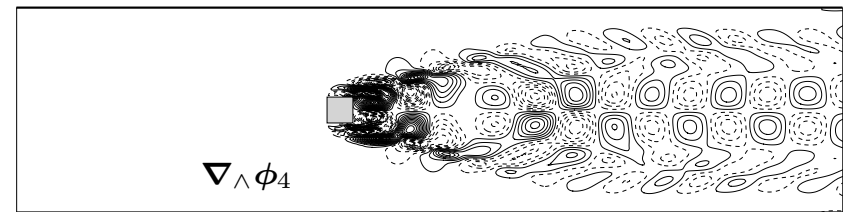
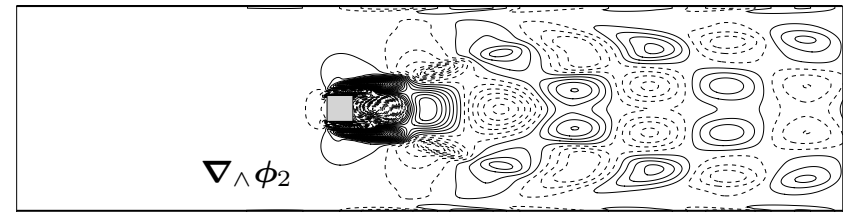
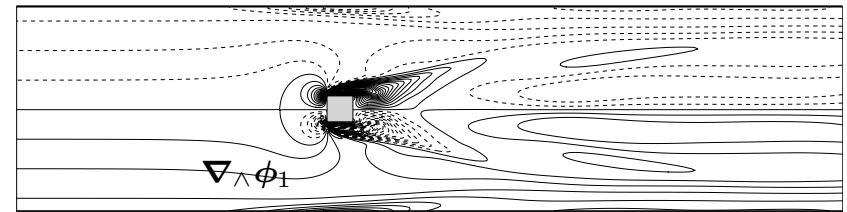
III - Improvement of the functional subspace

► **Second test case : 2D NSE equations** $Re_1 = 100 \rightarrow Re_2 = 200$ ($\Phi^{Re_1} \cdot \Phi^{Re_2} \approx 0.5$)

Initial basis, $Re_1 = 100$

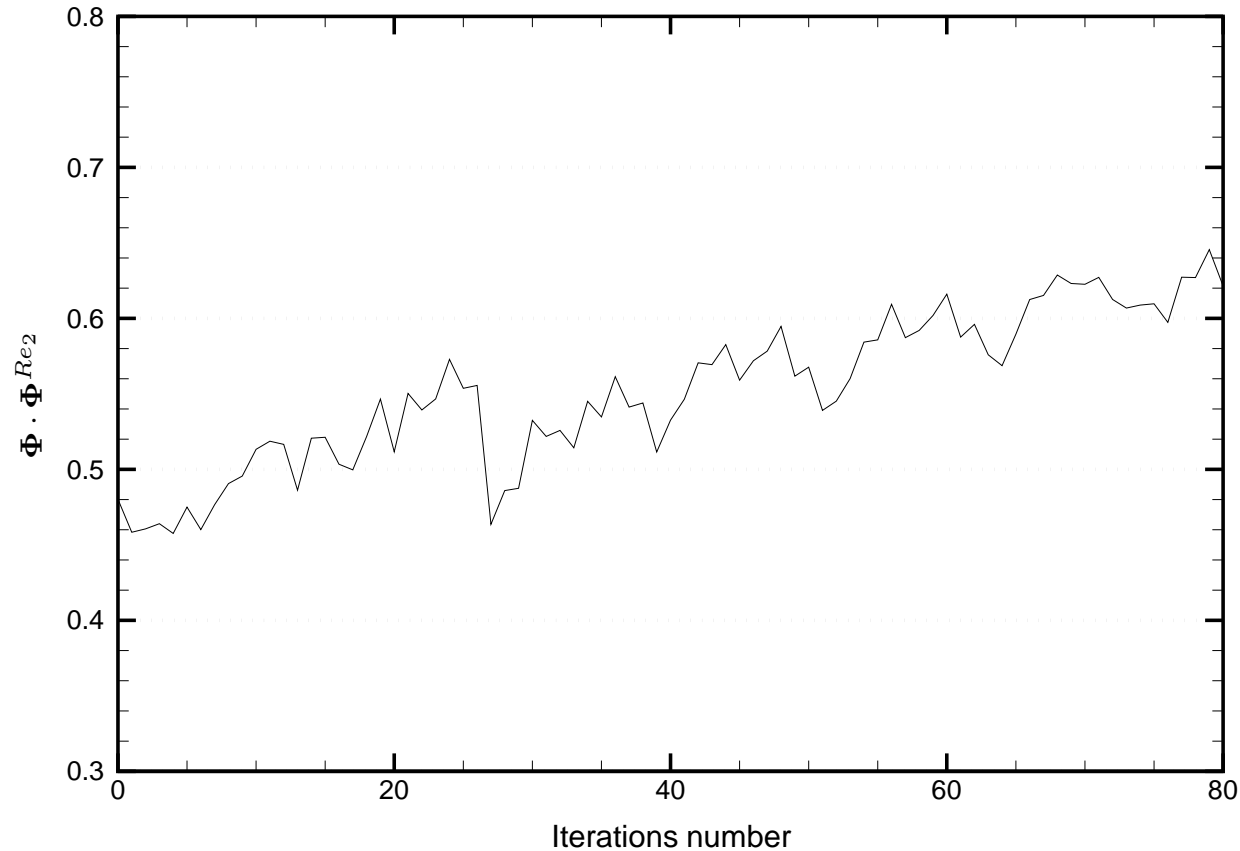


"Target" basis, $Re_2 = 200$



III - Improvement of the functional subspace

- **Second test case** : 2D NSE equations $Re_1 = 100 \rightarrow Re_2 = 200$ ($\Phi^{Re_1} \cdot \Phi^{Re_2} \approx 0.5$)



↪ No convergence...

III - Improvement of the functional subspace

► Observations

- the decomposition $U'(\mathbf{x}, t) = \tau \mathbf{R}(\mathbf{x}, t)$ is used to stabilize the ROM
↪ Very good results for NSE
- the decomposition $U'(\mathbf{x}, t) = \tau \mathbf{R}(\mathbf{x}, t)$ is used to improve POD basis
↪ Very good results for Burgers, quite bad results for NSE

► Possible explanation

- the decomposition $U'(\mathbf{x}, t) = \tau \mathbf{R}(\mathbf{x}, t)$ is only valid for
↪ Small values of $U'(\mathbf{x}, t)$ (for instance, non resolved POD modes).
↪ Can we find a good approximation τ of the elementary Green's function? Not sure...

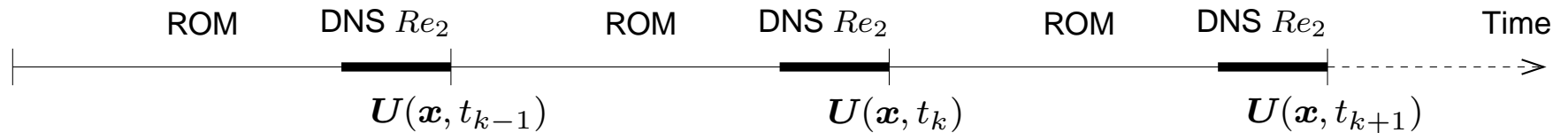
► Future works

- Look for an other decomposition for the missing scales $U'(\mathbf{x}, t)$
↪ $U'(\mathbf{x}, t) = M(t)\mathbf{R}(\mathbf{x}, t)$, where $M \in \mathbb{R}^{3 \times 3}$

III - Improvement of the functional subspace

▷ **Method 2 : hybrid ROM-DNS method to adapt the functional subspace $\Phi_n(\mathbf{x})$**

○ **Database modification** : statistics evolution $\Rightarrow \varphi : \Phi^{(k)} \mapsto \Phi^{(k+1)}$



1. Database modification $[U(\mathbf{x}, t_1) U(\mathbf{x}, t_2) \dots U(\mathbf{x}, t_{N_r})]$

$$\tilde{U}^{[1, \dots, N_r]}(\mathbf{x}, t_k) = \sum_{n=1}^{N_r} a_n(t_k) \phi_n(\mathbf{x}),$$

One snapshot modification using few DNS iterations

$$U(\mathbf{x}, t_s) = \tilde{U}^{[1, \dots, N_r]}(\mathbf{x}, t_s) + U_s^\perp(\mathbf{x}, t_s).$$

In a general way

$$\tilde{U}(\mathbf{x}, t_k) = \tilde{U}^{[1, \dots, N_r]}(\mathbf{x}, t_k) + \delta_{ks} U^\perp(\mathbf{x}, t_s),$$

III - Improvement of the functional subspace

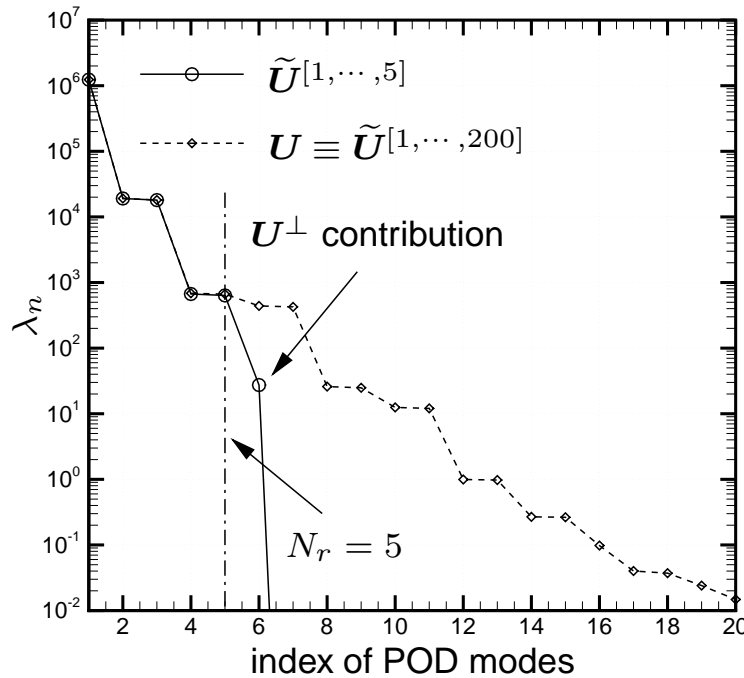
2 Modification temporal correlations tensor

$$\begin{aligned}
 C(t_k, t_l) &= (\mathbf{U}(\mathbf{x}, t_k), \mathbf{U}(\mathbf{x}, t_l))_{\Omega} \\
 &= \left(\sum_{i=1}^{N_r} a_i(t_k) \phi_i(\mathbf{x}) + \mathbf{U}^{\perp}(\mathbf{x}, t_k), \sum_{j=1}^{N_r} a_j(t_l) \phi_j(\mathbf{x}) + \mathbf{U}^{\perp}(\mathbf{x}, t_l) \right)_{\Omega} \\
 &= \sum_{i=1}^{N_r} \sum_{j=1}^{N_r} a_i(t_k) a_j(t_l) \underbrace{(\phi_i(\mathbf{x}), \phi_j(\mathbf{x}))_{\Omega}}_{=\delta_{ij}} + (\mathbf{U}^{\perp}(\mathbf{x}, t_k), \mathbf{U}^{\perp}(\mathbf{x}, t_l))_{\Omega} \\
 &\quad + \sum_{i=1}^{N_r} a_i(t_k) \underbrace{(\phi_i(\mathbf{x}), \mathbf{U}^{\perp}(\mathbf{x}, t_l))_{\Omega}}_{=0} + \sum_{j=1}^{N_r} a_j(t_l) \underbrace{(\mathbf{U}^{\perp T}(\mathbf{x}, t_k), \phi_j(\mathbf{x}))_{\Omega}}_{=0}.
 \end{aligned}$$

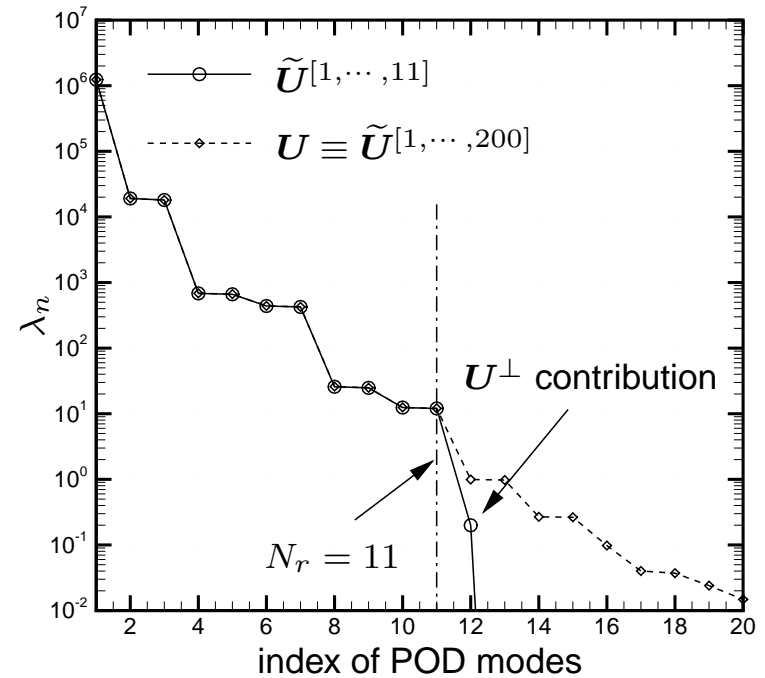
Final approximation

$$C(t_k, t_l) = \sum_{i=1}^{N_r} a_i(t_k) a_i(t_l) + \delta_{ks} \delta_{ls} \int_{\Omega} \sum_{i=1}^{n_c} U^{\perp i}(\mathbf{x}, t_s) U^{\perp i}(\mathbf{x}, t_s) d\mathbf{x}.$$

III - Improvement of the functional subspace



$N_r = 5$



$N_r = 11$

Fig. : Comparison of the temporal correlation tensor eigenvalues evaluated from the exact field, U , and from the N_r -modes approximated one, $\tilde{U}[1, \dots, N_r]$.

↪ Very good approximation, and very low costs method!

III - Improvement of the functional subspace

3 Functional subspace adaptation

$$\phi_k^{(n+1)}(\mathbf{x}) = \frac{1}{\lambda_k^{(n+1)}} \sum_{j=1}^{N_r} \tilde{U}^{(n)}(\mathbf{x}, t_j) a_k^{(n+1)}(t_j)$$

$$\phi_k^{(n+1)}(\mathbf{x}) = \frac{1}{\lambda_k^{(n+1)}} \sum_{i=1}^{N_r} \sum_{j=1}^{N_r} a_k^{(n+1)}(t_j) a_i^{(n)}(t_j) \phi_i^{(n)}(\mathbf{x}) + \frac{1}{\lambda_k} \mathbf{U}^\perp{}^{(n)}(\mathbf{x}, t_s) a_k^{(n+1)}(t_s).$$

$$\phi_k^{(n+1)}(\mathbf{x}) = \sum_{i=1}^{N_r} K_{ki}^{(n+1)} \phi_i^{(n)}(\mathbf{x}) + \mathbf{S}_k^{(n+1)}(\mathbf{x}).$$

Taken $S^{(n+1)}$ with elements $S_{ij}^{(n+1)} = S_i^j{}^{(n+1)}$, the actualized basis is obtained using the linear application $\varphi : \mathbb{R}^n \times \mathbb{R}^n \mapsto \mathbb{R}^n \times \mathbb{R}^n$ defined as

$$\varphi : \phi^{(n)} \mapsto \phi^{(n+1)} = \phi^{(n)} K^{(n+1)} + S^{(n+1)}$$

Incrementation $n = n + 1$.

III - Improvement of the functional subspace

► Results for a dynamical evolution from $Re_1 = 100$ to $Re_2 = 200$

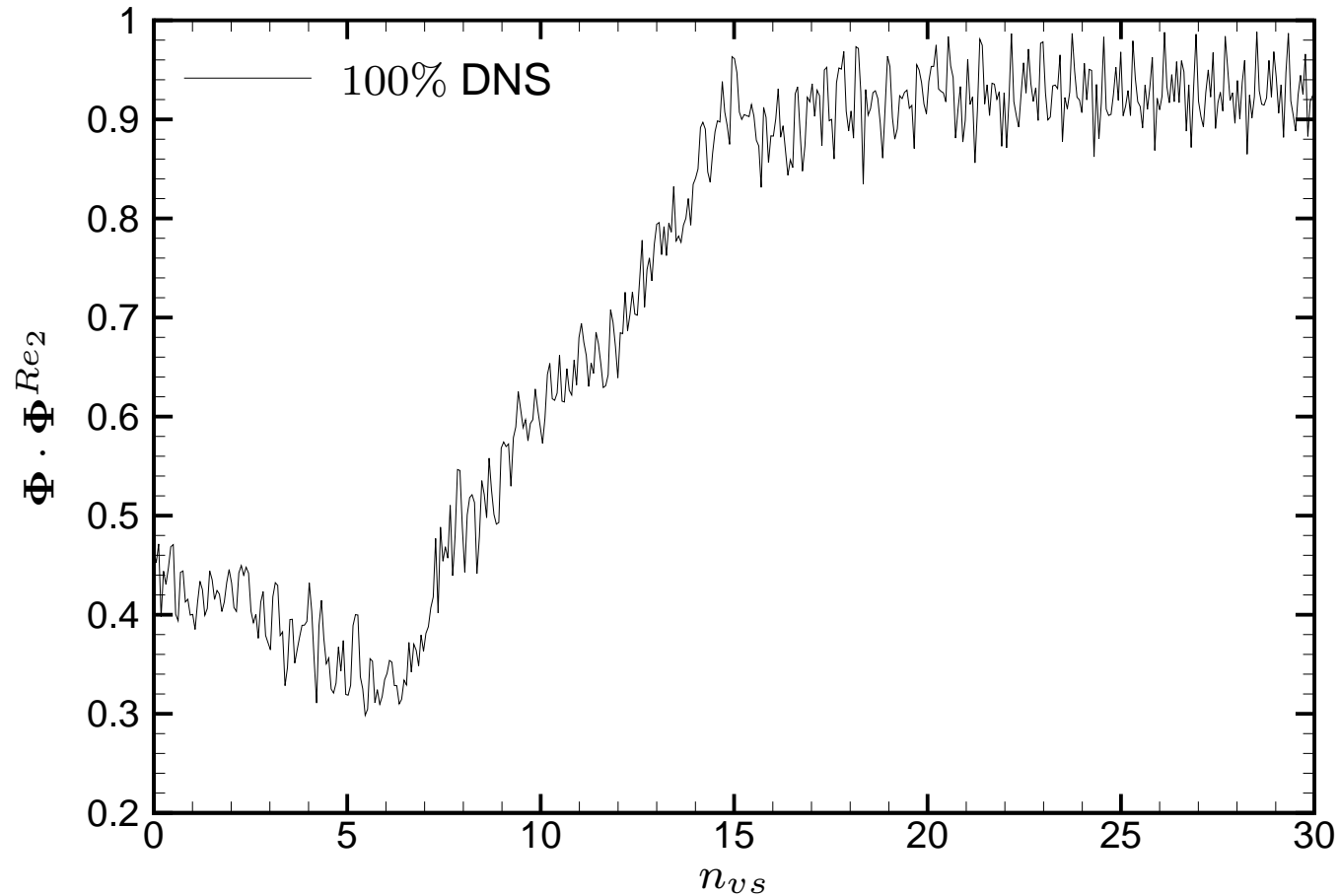


Fig. : temporal evolution of the POD basis

III - Improvement of the functional subspace

► Results for a dynamical evolution from $Re_1 = 100$ to $Re_2 = 200$

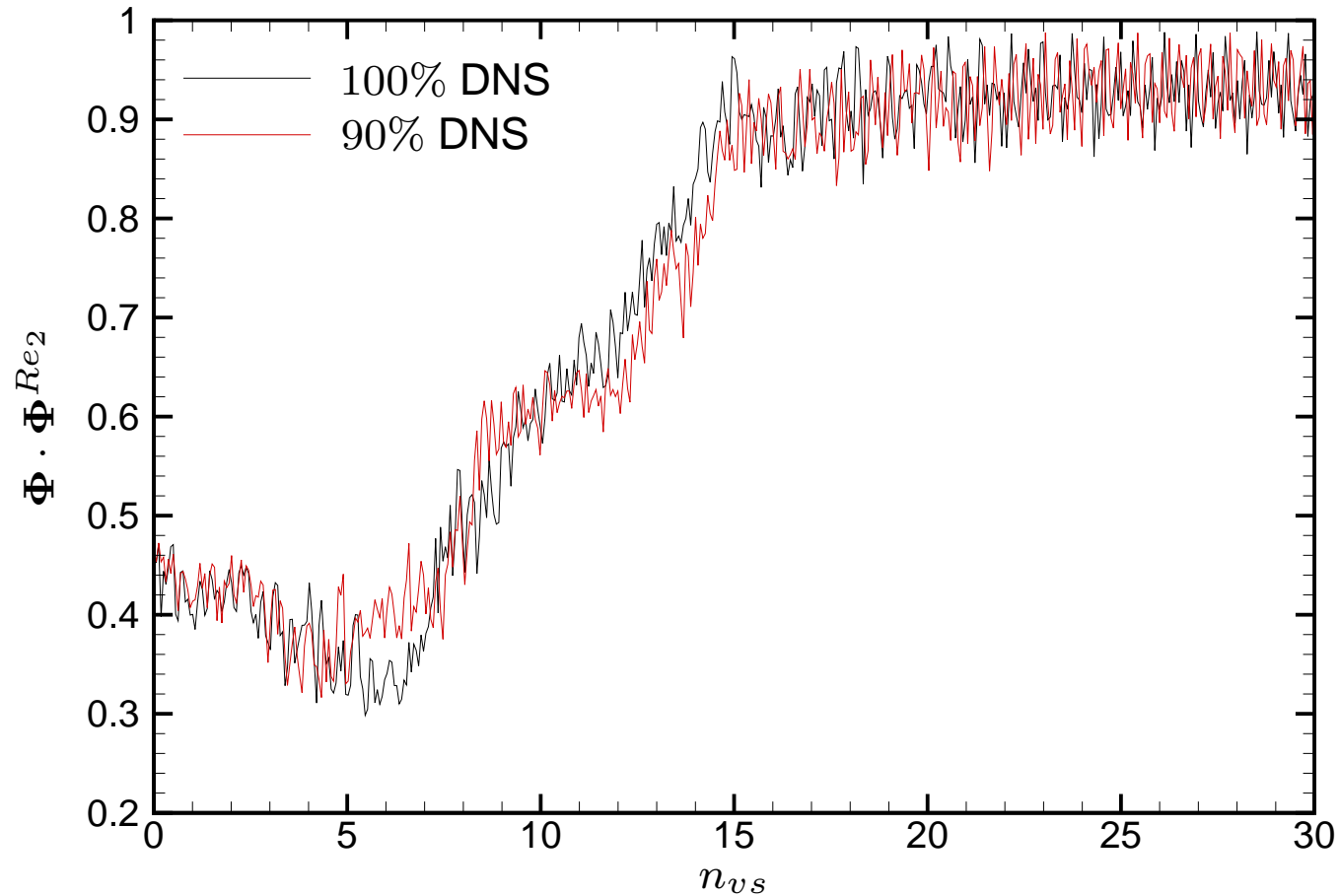


Fig. : temporal evolution of the POD basis

III - Improvement of the functional subspace

► Results for a dynamical evolution from $Re_1 = 100$ to $Re_2 = 200$

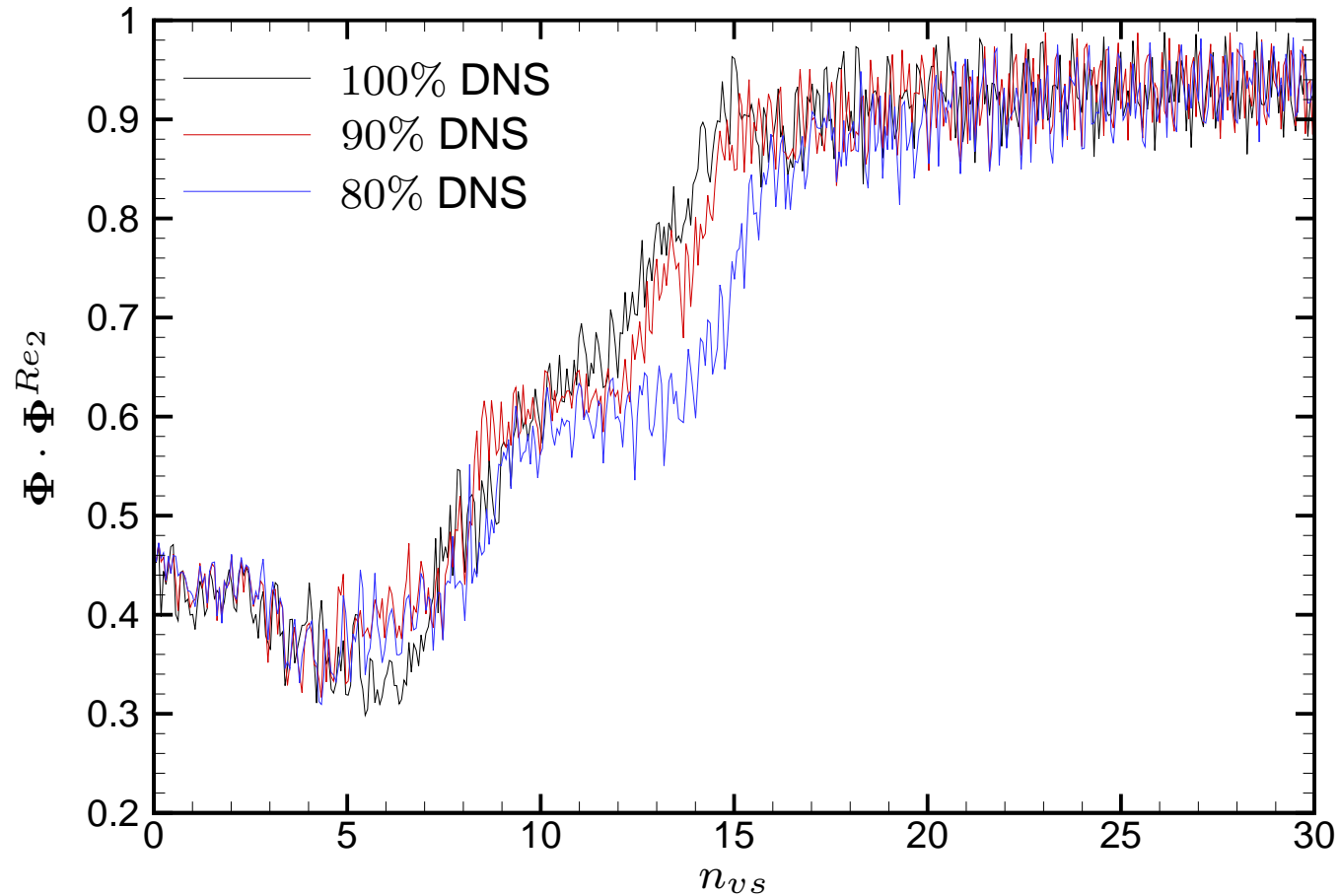


Fig. : temporal evolution of the POD basis

III - Improvement of the functional subspace

► Results for a dynamical evolution from $Re_1 = 100$ to $Re_2 = 200$

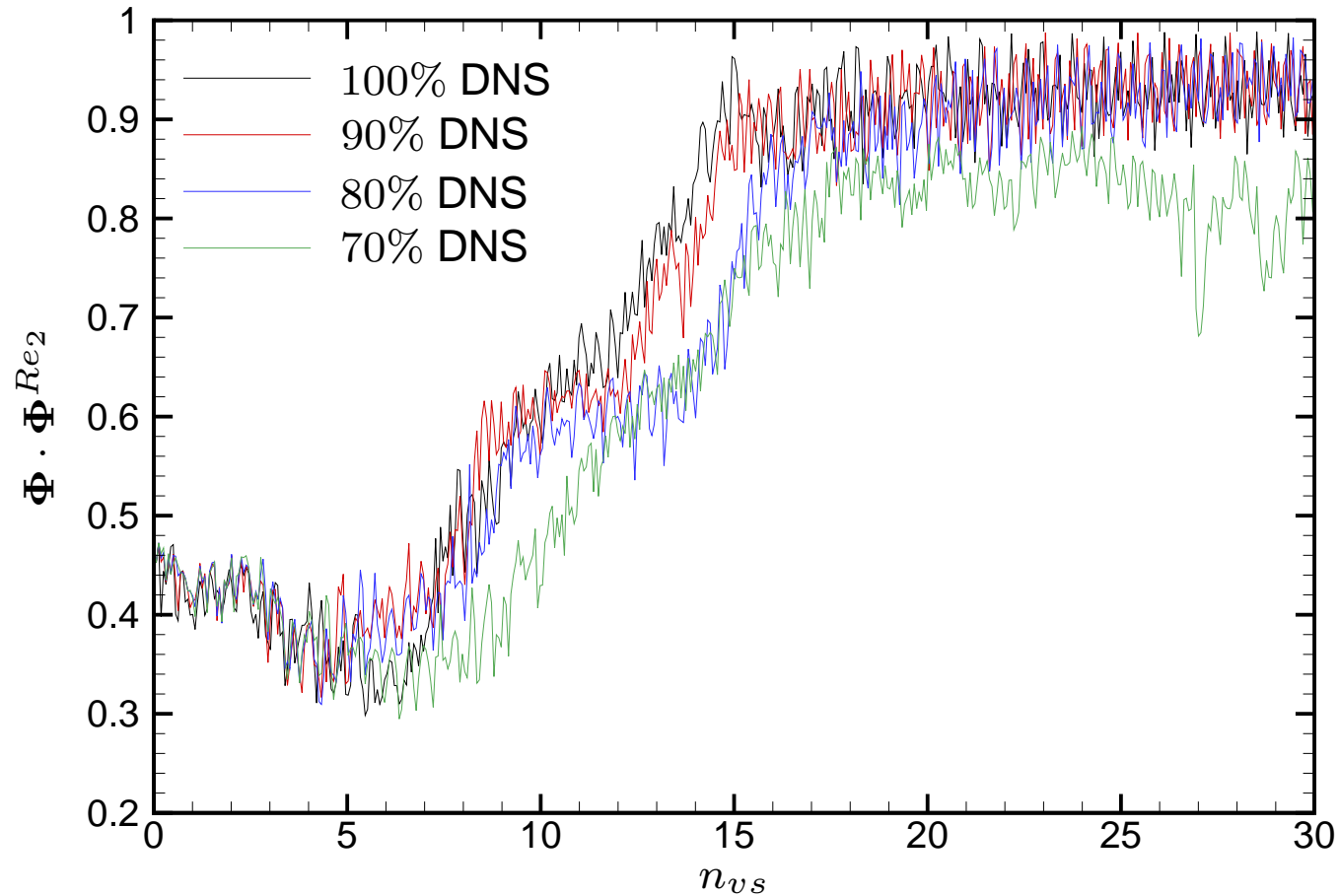


Fig. : temporal evolution of the POD basis

III - Improvement of the functional subspace

► Results for a dynamical evolution from $Re_1 = 100$ to $Re_2 = 200$

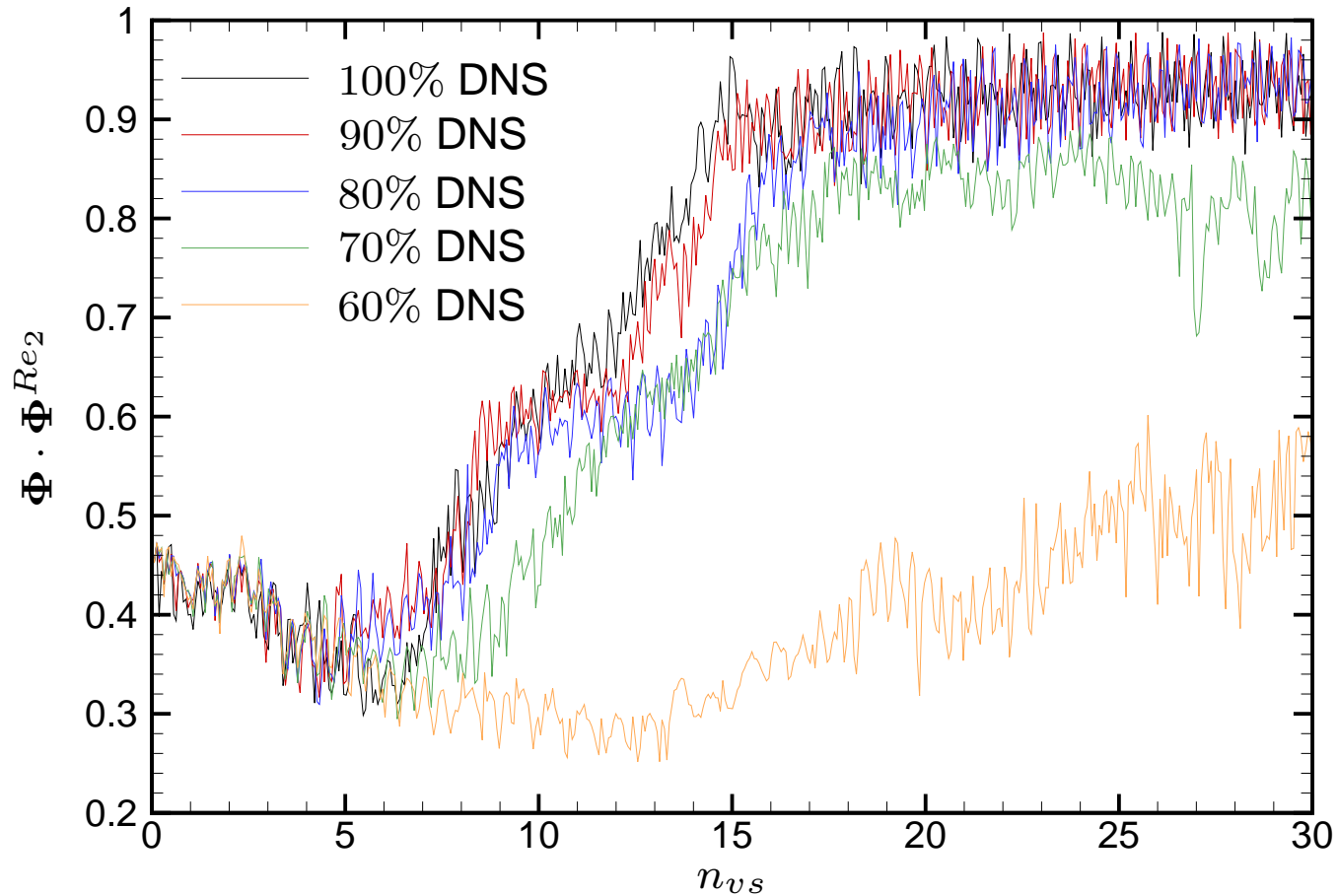


Fig. : temporal evolution of the POD basis

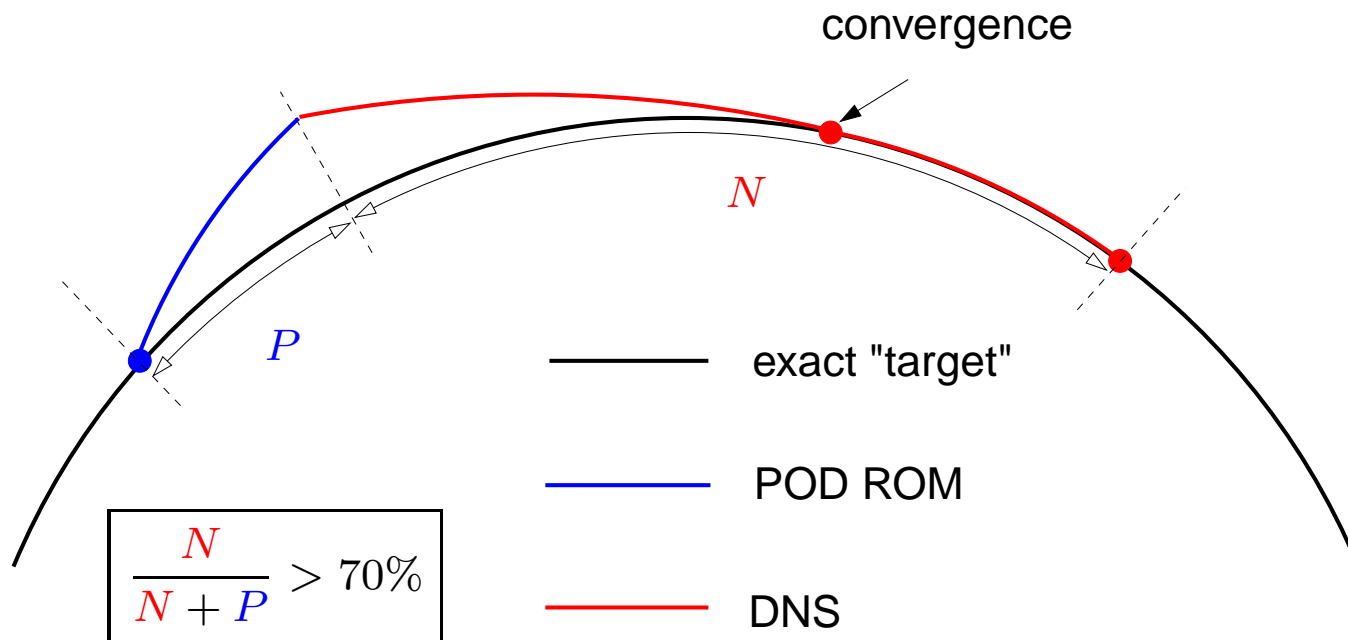
III - Improvement of the functional subspace

► Observations

● Results are very good if a sufficient amount of DNS is performed

↪ Good for a percentage $\frac{DNS}{DNS+PODROM}$ greater than 70%

► Possible explanation



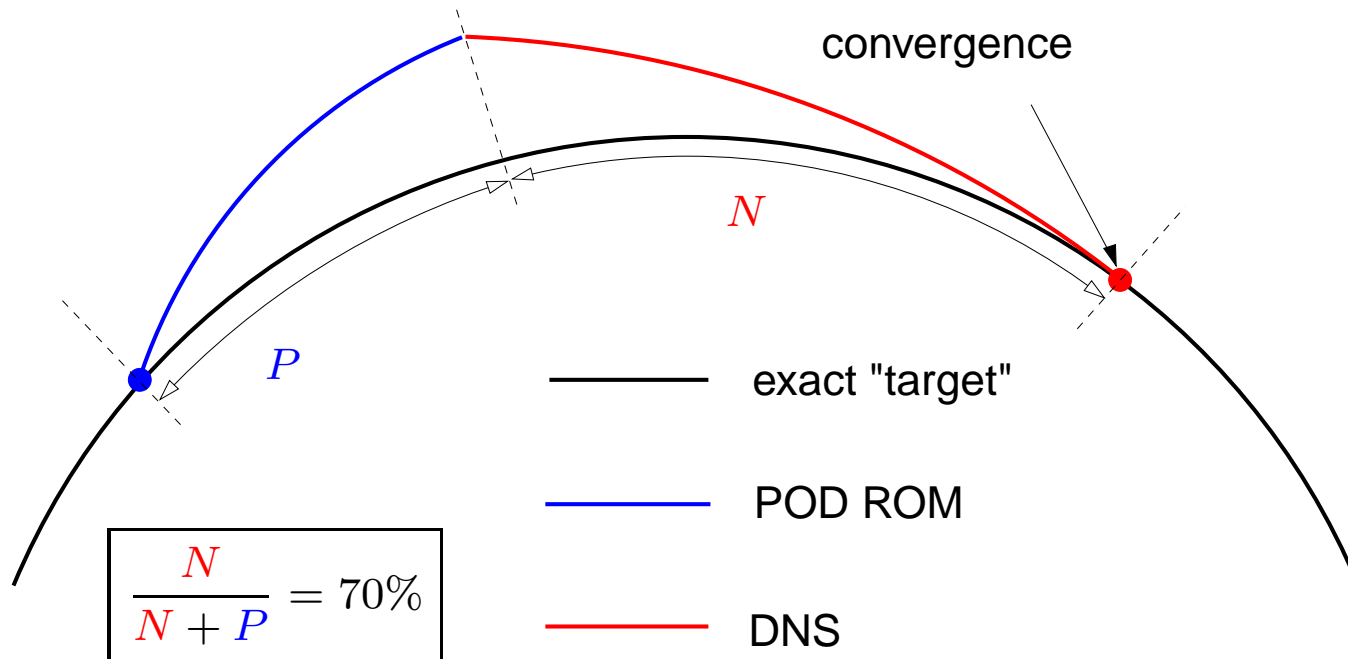
III - Improvement of the functional subspace

► Observations

● Results are very good if a sufficient amount of DNS is performed

↪ Good for a percentage $\frac{DNS}{DNS+PODROM}$ greater than 70%

► Possible explanation



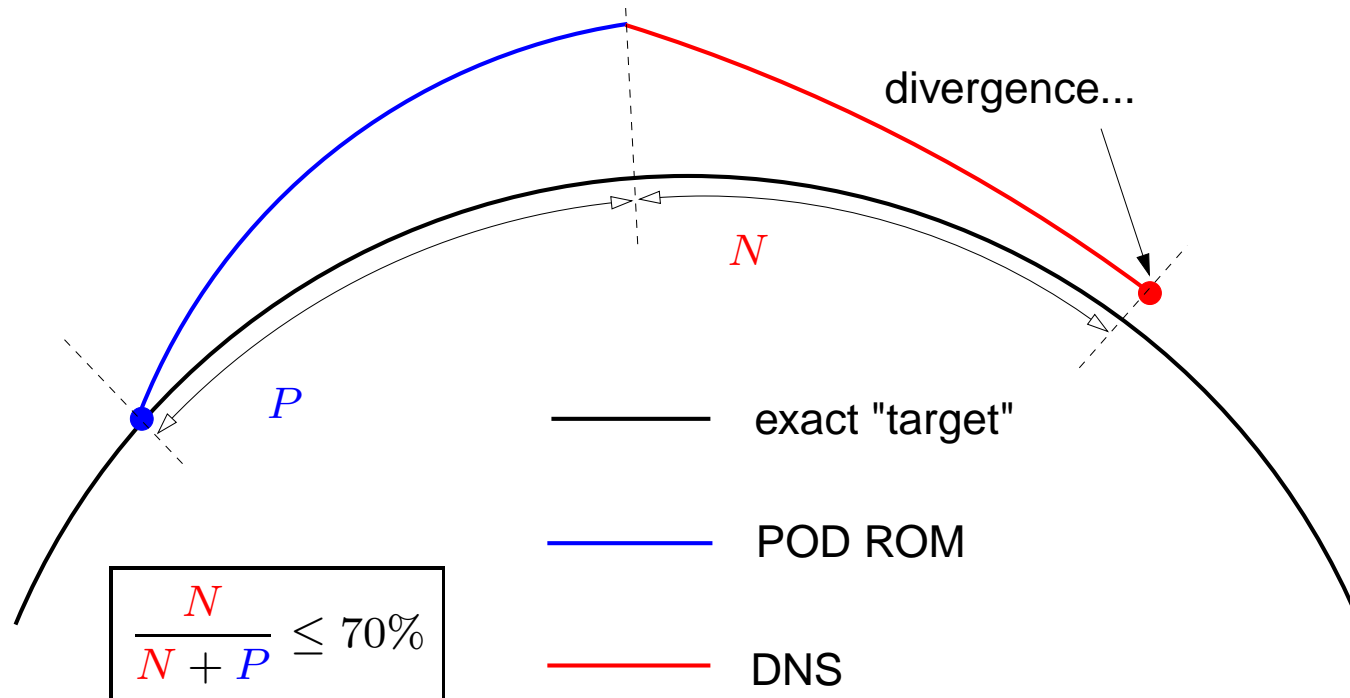
III - Improvement of the functional subspace

► Observations

● Results are very good if a sufficient amount of DNS is performed

↪ Good for a percentage $\frac{DNS}{DNS+PODROM}$ greater than 70%

► Possible explanation



Conclusions

▷ A pressure extended Reduced Order Model

- The pressure is naturally included in the ROM \Rightarrow no modelisation of pressure term...
- ... but need of modelisation interaction with non resolved modes (dissipation)

▷ Stabilization of Reduced Order Models based on POD

- Add some residual modes \Rightarrow Good results
- SUPG and VMS methods \Rightarrow Very good results

▷ Try to improve the functional subspace

- Improvement using POD-NSE residuals (Krylov like method)
 - \hookrightarrow Very good for 1D burgers equation but quite poor results for 2D NSE equations
 - \hookrightarrow Problem with the continuity equation ?
 - \hookrightarrow Missing scales \neq "fine scales" \Rightarrow approximation $U'(\boldsymbol{x}, t) = \tau \boldsymbol{R}(\boldsymbol{x}, t)$ not good!
- Database modification : an hybrid DNS/ROM method
 - \hookrightarrow Fast evaluation of temporal correlations tensor
 - \hookrightarrow Linear actualization of the POD basis
 - \hookrightarrow DNS must correct ROM \Rightarrow good results for amount of DNS greater than 70%